Geol. Mag. **156** (*1*), *2019, pp. 39–61* © *Cambridge University Press 2017*
doi:10.1017/S0016756817000772

The Thrace Basin and the Black Sea: the Eocene–Oligocene marine connection

ARAL I. OKAY*†‡, ERCAN ÖZCAN†, AYNUR HAKYEMEZ§, MUZAFFER SIYAKO¶, GÜRSEL SUNAL† & ANDREW R.C. KYLANDER-CLARK||

*Istanbul Technical University, Eurasia Institute of Earth Sciences, Maslak 34469, Istanbul, Turkey
†Istanbul Technical University, Faculty of Mines, Department of Geology, Maslak 34469, Turkey
§General Directorate of Mineral Research and Expolaration (MTA), Department of Geological Research, 06800 Ankara, Turkey
¶3S Kale Enerji Üretim A. Ş., Güngören, Istanbul, Turkey
||University of California Santa Barbara, Department of Earth Sciences, Santa Barbara, CA 93106 USA

(*Received* 14 February 2017; *accepted* 13 August 2017)

Abstract – The Late Cretaceous – Recent West Black Sea Basin and the Eocene–Oligocene Thrace Basin are separated by the Strandja arch comprising metamorphic and magmatic rocks. Since Late Cretaceous time the Strandja arch formed a palaeo-high separating the two basins which accumulated clastic sediment of >9 km thickness. During late Eocene – early Oligocene time the marine connection between these basins existed through the Çatalca gap west of Istanbul. The Çatalca gap lies on the damage zone of a major Cretaceous strike-slip fault; it formed a 15 km wide marine gateway, where carbonate-rich sediments of thickness *c.* 350 m were deposited. The sequence consists of upper Eocene shallow marine limestones (SBZ18-20) overlain by upper Eocene – lower Oligocene (P16-P19 zones) pelagic marl with a rich fauna of planktonic foraminifera; the marls are intercalated with 31–32 Ma acidic tuff and calc-arenite beds. The Çatalca gap is bounded in the west by a major normal fault, which marks the eastern boundary of the Thrace Basin. Seismic reflection profiles, well data and zircon U–Pb ages indicate that the Thrace Basin sequence west of the fault is late Eocene – middle Oligocene (37–27 Ma) in age and that the fault has accommodated 2 km of subsidence. Although there was a marine connection between the West Black Sea and Thrace basins during late Eocene – early Oligocene time, no significant exchange of clastic sediment took place. Sedimentation in the Çatalca gap ended abruptly during early Oligocene time by uplift, and this eventually led to the paralic conditions in the Thrace Basin.

Keywords: Turkey, Cenozoic stratigraphy, foraminifera, zircon U–Pb geochronology, seismic reflection

1. Introduction

The West Black Sea Basin opened during Late Cretaceous time as a back-arc basin with thinned continental and oceanic crust to the north of the Pontide magmatic arc (e.g. Robinson *et al.* 1996; Nikishin *et al.* 2015*a*). The basin underwent continuous subsidence resulting in a sedimentary thickness of >14 km. The adjacent Thrace Basin, 300 km by 300 km in area, is younger; it is filled with Eocene–Oligocene clastic strata, reaching a thickness of 9 km in its central part (Kopp, Pavoni & Schindler, 1969; Doust & Arıkan, 1974; Turgut, Türkarslan & Perinçek, 1991). These two hydrocarbon-bearing basins are separated by the Strandja Massif, which is made up of metamorphic and plutonic rocks (Fig. 1). During Cenozoic time most of the Strandja Massif formed a land area of low relief undergoing minor erosion, as reflected in the Late Cretaceous apatite fission-track ages (Cattò *et al.* 2017). The only region where the Eocene–Oligocene sequences of the Black Sea and Thrace Basin are in contact is the Çatalca area west of Istanbul. This 20 km wide area, referred to here as the Çatalca gap, also has a special tectonic significance as it corresponds to the location of a major Cretaceous strike-slip fault, the West Black Sea Fault, separating the Strandja Massif and the Istanbul Zone (Okay, Şengör & Görür, 1994). During the opening of the West Black Sea Basin, the Istanbul Zone was translated southwards from its original position south of the Odessa shelf along the West Black Sea Fault. The West Black Sea Fault extends onshore to the Çatalca gap, where it is concealed by Eocene and Oligocene strata (Fig. 2).

The Çatalca gap is a broad area of low relief between the Strandja Massif and the Istanbul Zone. The oldest Tertiary sediments in the Çatalca gap are upper Eocene shallow-marine limestones of the Soğucak Formation (Figs 2, 3; Less, Özcan & Okay, 2011). The limestones are unconformably overlain by the upper Eocene – lower Oligocene pelagic marls with acidic tuff

‡Author for correspondence: okay@itu.edu.tr

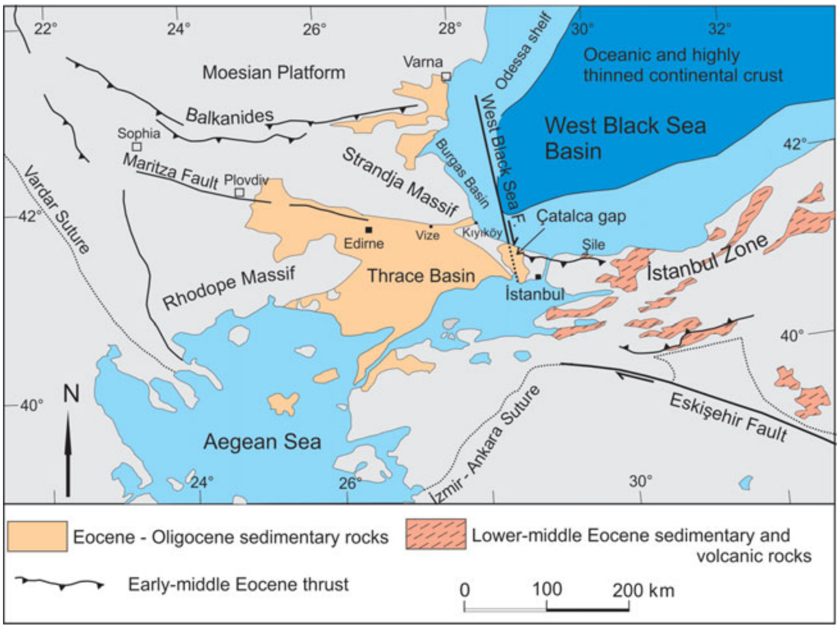

Figure 1. (Colour online) Map of the Black Sea – northern Aegean region showing the locations of the Thrace and West Black Sea basins.

horizons, known as the İhsaniye Formation (Yurtsever & Çağlayan, 2002; Gedik *et al.* 2014), which crop out over wide areas in the Çatalca gap (Fig. 2). The Çatalca gap is bounded in the east by a palaeo-high made up of the Carboniferous sandstones of the Istanbul Zone and in the west by the Çatalca ridge, which also constitutes the boundary between the Thrace Basin and Black Sea realm. The Çatalca ridge represents the southernmost spine of the Strandja Massif and consists of pre-Tertiary metamorphic and granitic rocks, which are overlain on its northeastern side by upper Eocene shallow-marine limestones (Fig. 2; Less, Özcan & Okay, 2011). In the SW the Çatalca ridge is bounded by a major normal fault, the Çakıl Fault, which formed a major hinge zone during Oligocene time. Seismic sections and petroleum wells indicate the existence of a regressive Eocene–Oligocene clastic sequence, several kilometres thick, of the Thrace Basin SW of the Çakıl Fault. We have investigated the stratigraphic units in the Çatalca gap and in the neighbouring Thrace Basin using geological mapping, micropalaeontology, zircon U–Pb geochronology and seismic reflection.

2. Methods

2.a. Planktonic foraminifera

Sixty marl samples collected from six stratigraphic sections were studied for planktonic foraminifera. Samples were disaggregated by diluted hydrogen peroxide (30 %) for obtaining isolated specimens. Planktonic foraminiferal assemblages are abundant, well diversified and preserved in all samples. Taxonomic analyses are based mainly on Pearson *et al.* (2006) and the biozonation follows Berggren *et al.* (1995).

2.b. Larger benthic foraminifera

Larger benthic foraminifera (nummulitids, orthophragminids) have been sampled from the Eocene and lower Oligocene shallow – deep-marine strata. The loose specimens, isolated from the marl and limestone, have been sectioned through the equatorial and axial planes for taxonomic studies. The biostratigraphic scheme (SBZ zones) follows Serra-Kiel *et al.* (1998), Less & Özcan (2012) and Papazzoni *et al.* (2017).

2.c. Mineral separation, preparation and laser ablation ICP-MS zircon dating

Zircon fractions from rock samples were separated in Istanbul Technical University using standard mineral separation procedures. This included crushing whole-rock samples to sand-size grains, sieving, repeated rinsing and cleansing of samples in water and acetone and passing the samples through a Frantz magnetic separator. For zircon separation we used heavy liquids followed by handpicking under stereographic microscope. The zircons were mounted in epoxy and were polished in the Istanbul Technical University. Cathodoluminescence (CL) images of the polished zircons were taken on a Zeiss Evo 50 EP scanning electron microscope at the Hacettepe University in Ankara. Zircons were analysed using laser ablation inductively coupled plasma mass spectrometry (LA-ICP-MS) at the University of California, Santa Barbara (Kylander-Clark, Hacker & Cottle, 2013). For session-specific details of the method employed here, see Okay *et al.* (2014). Long-term reproducibility in secondary reference materials is <2 % and, as such, should be used when comparing ages obtained within this analytical session to ages elsewhere. Where applicable, for age calculations 2 % uncertainty is shown in brackets

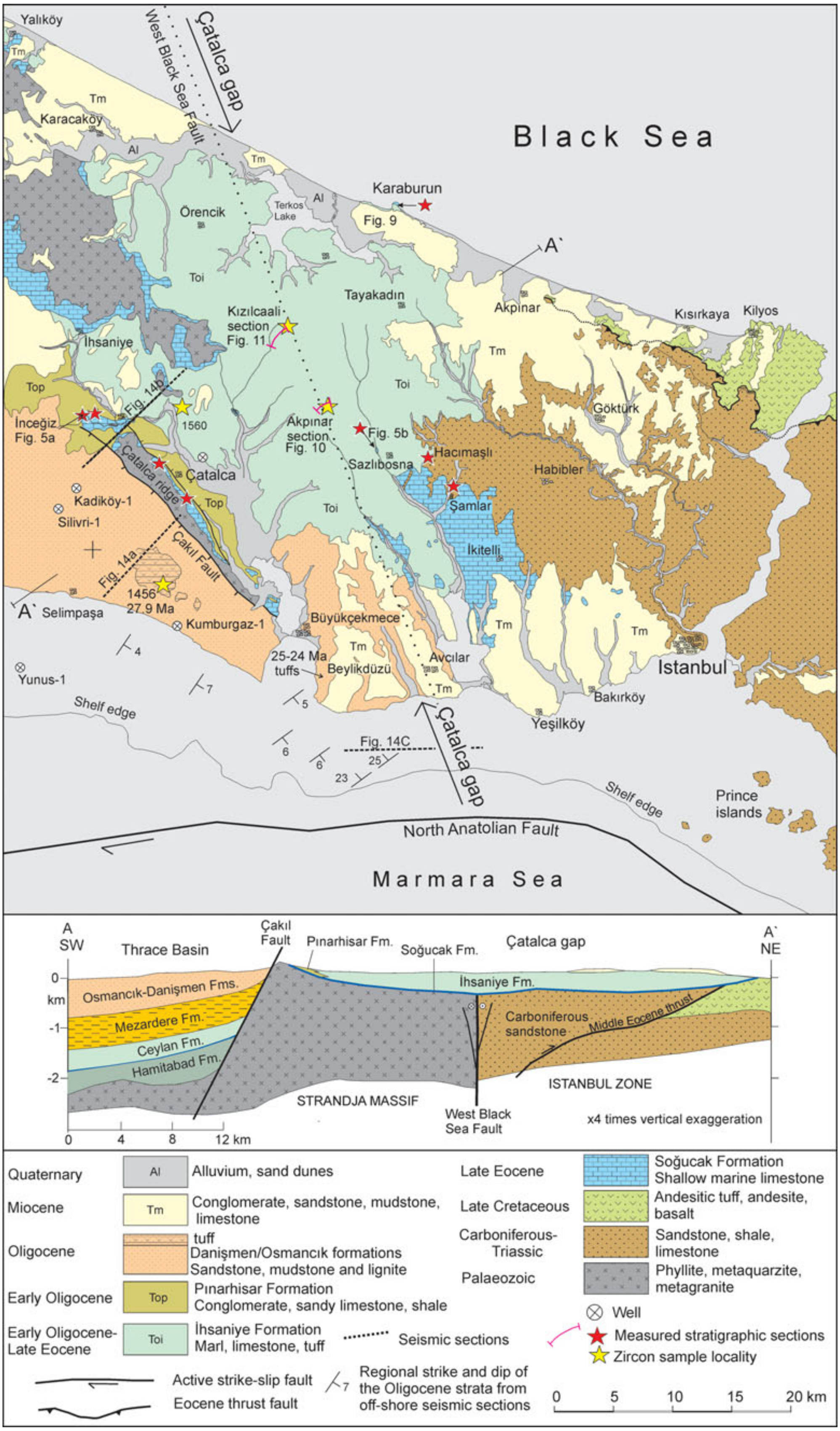

Figure 2. (Colour online) Geological map and cross-section of the Çatalca gap west of Istanbul (based on Akartuna, 1953; Yurtsever & Çağlayan, 2002; Gedik *et al.* 2014 and our own geological mapping). For location see Figure 1.

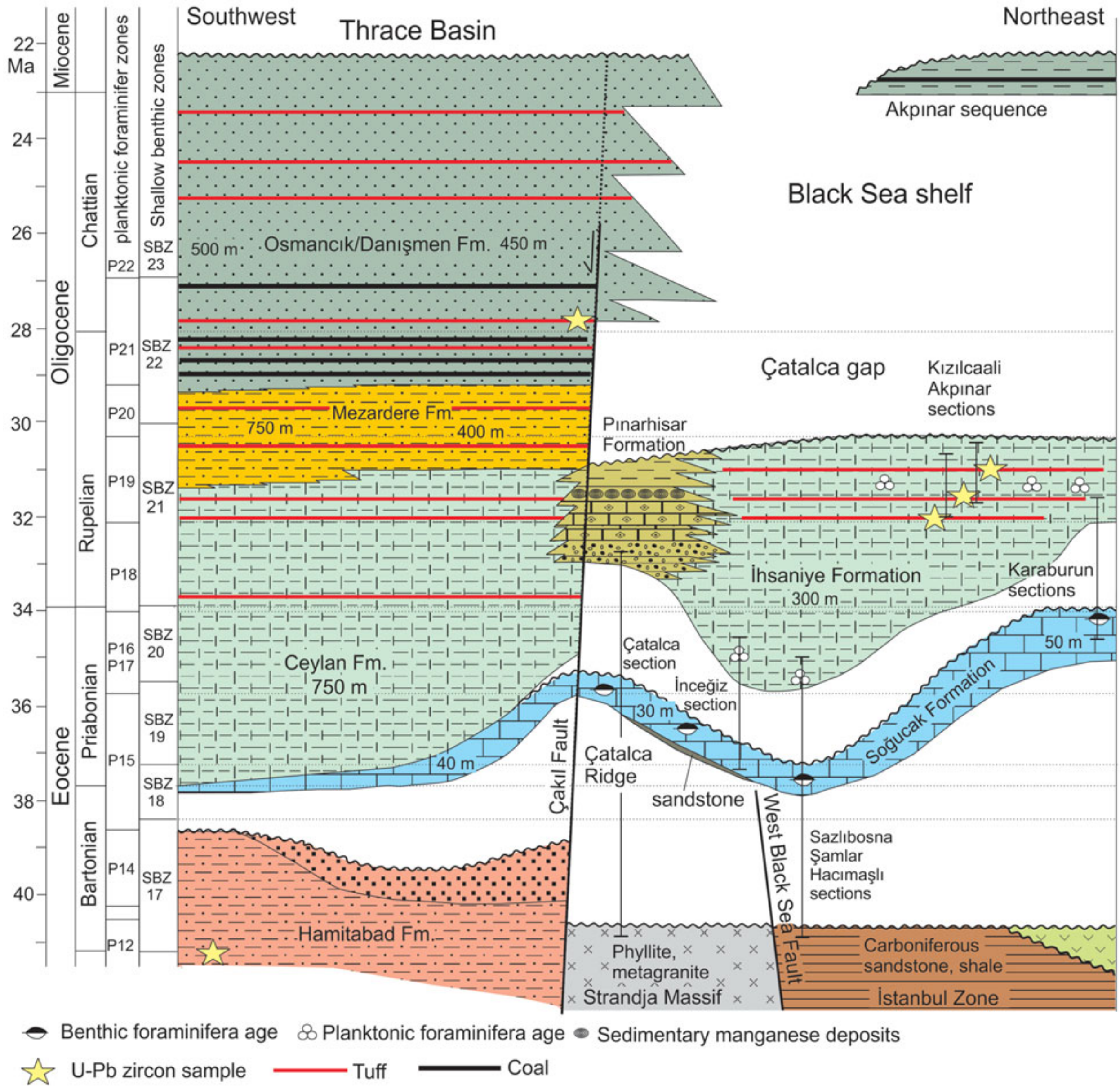

Figure 3. (Colour online) Generalized stratigraphic section showing the relation of the Eocene–Oligocene units in the Thrace Basin and the Çatalca gap. The timescale is from Gradstein *et al.* (2012).

following the analytical uncertainty. The analytical data are given in online Supplementary Tables S1–S5, available on the Cambridge Journals Online website (http://journals.cambridge.org/geo).

3. The Eocene–Oligocene sequence in the Çatalca gap

The Tertiary stratigraphy in the region between the Çatalca ridge and the Black Sea consists of shallow-marine upper Eocene limestones overlain disconformably by Oligocene and Miocene sequences (Figs 2, 3).

3.a. Upper Eocene shallow-marine carbonates: the Soğucak Formation

The Soğucak Formation consists of thickly bedded to massive, white to light-grey shallow-marine limestone, 5–60 m thick, with solitary corals, bivalves, algae, bryzoans and larger benthic foraminifera (Less, Özcan & Okay, 2011). In the west it lies unconformably above the metamorphic rocks of the Çatalca ridge, in the east above the Carboniferous sandstones and in the north on the Black Sea coast possibly on the Upper Cretaceous volcanic rocks (Fig. 2). The Eocene marine transgression occurred on a rugged, tectonically active topography, as shown by Neptunian dykes in the metamorphic rocks of the Çatalca ridge filled by Eocene limestone penetrating up to 10 m below the contact (Fig. 4a; Less, Özcan & Okay, 2011). At some localities such as in the northern parts of the Çatalca ridge or above the Carboniferous sandstones, there is a sandstone horizon at the base of the Soğucak Formation.

The Soğucak Formation was studied in several sections, which include those described in Less, Özcan &

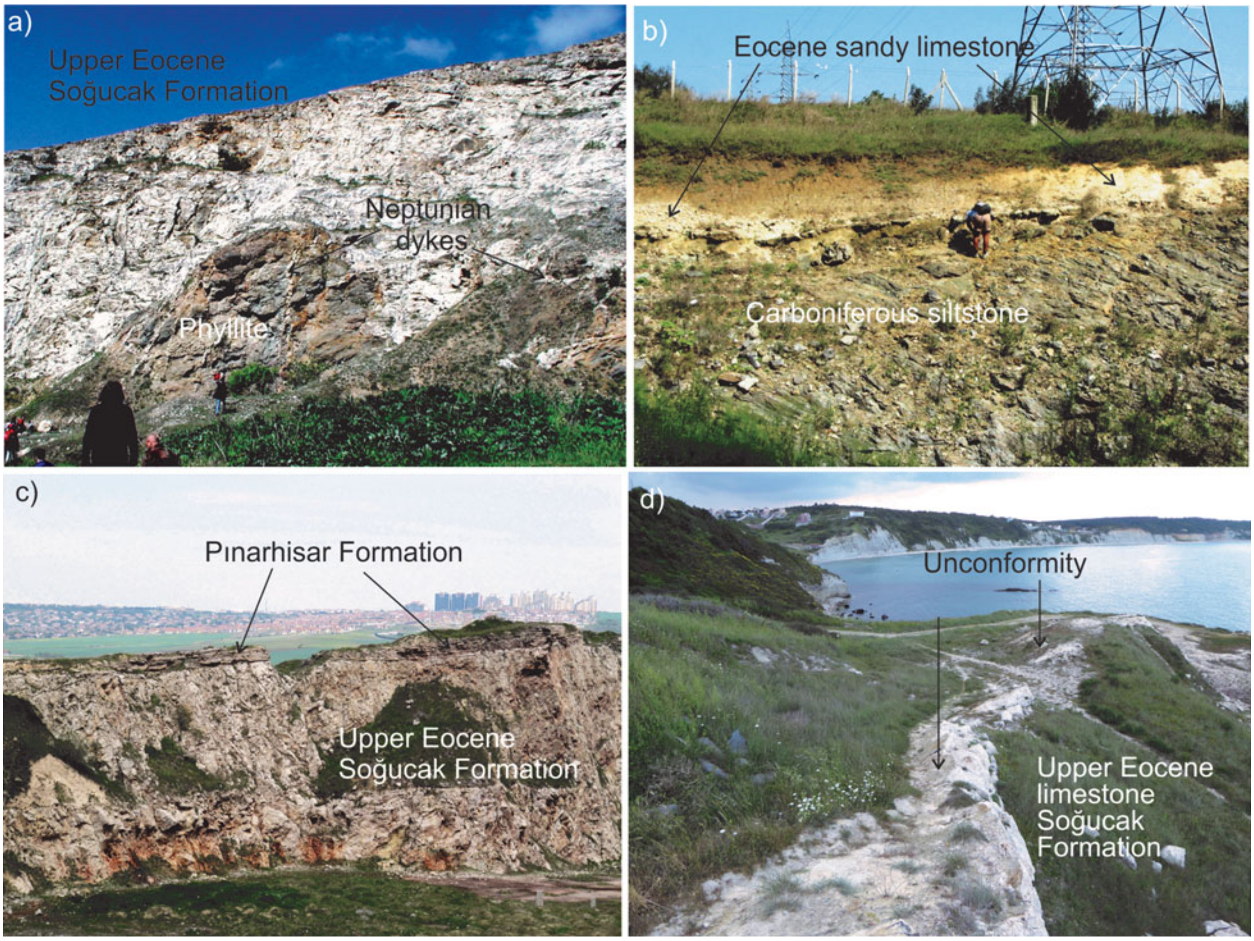

Figure 4. (Colour online) Field photographs of the Eocene–Oligocene sequences. (a) Upper Eocene (SBZ18–19) shallow-marine limestones of the Soğucak Formation lying unconformably over the phyllites of the Strandja Massif in the Çatalca ridge. Note the irregular unconformity surface and the Neptunian dykes filled with limestone. (b) Upper Eocene (SBZ18) sandy limestones lying unconformably above the Carboniferous siltstones in the Sazlıbosna section (cf. Fig. 5b). (c) Upper Eocene shallow-marine limestones of the Soğucak Formation overlain unconformably by the sandy, pebbly lagoonal limestones of the lower Oligocene Pınarhisar Formation, west of the Büyükçekmece Lake. (d) The unconformity above the upper Eocene reefal limestones in Karaburun. The Karaburun 1588 section was measured across this contact (cf. Fig. 5c). The cliffs in the background are formed of lower Oligocene marl. (e) Neptunian dyke in the reefal massive Eocene limestone in Karaburun. (f) White Oligocene calcareous siltstone lying unconformably over the massive Eocene limestones. The section 1590 in Figure 5d was measured across this contact. (g) The lower Oligocene sequence in Karaburun. The well-bedded pebbly sandy limestones on the left (Toi_1) are overlain by marls (Toi_2). (h) A block of upper Eocene limestone in the Oligocene sandy limestones.

Okay (2011) and a new section at Sazlıbosna (Figs 2, 5b). Larger benthic foraminifera from the Soğucak Formation were used to assign its age to shallow benthic zones SBZ18–20. In studies prior to 2012, SBZ18 was included in the middle Eocene (Bartonian; Serra-Kiel *et al.* 1998; Özcan *et al.* 2006); however, new magnetostratigraphic and biostratigraphic data indicate that the middle–upper Eocene boundary lies in the lower part of SBZ18 (in SBZ18A; e.g. Costa *et al.* 2013; Rodelli *et al.* 2016; Papazzoni *et al.* 2017). The age of the Soğucak Formation in the Çatalca gap and in most of the Thrace Basin is therefore predominantly late Eocene.

Biostratigraphic data from the Soğucak Formation indicate that the Eocene sea first flooded the centre of the Çatalca gap and later its margins. In the Sazlıbosna section Carboniferous siltstones are unconformably overlain by 6 m thick sandy, pebbly limestone rich in foraminifera, including *Discocyclina radians*, *Discocyclina augustae*, *Heterostegina armenica armenica*, *Operculina* ex. gr. *gomezi*, *Assilina* ex. gr. *schwageri-alpina* and *Orbitoclypeus varians*, which indicate an age around the middle–late Eocene (Bartonian–Priabonian) boundary (SBZ18A; Figs 4b, 5b, 6). In the nearby Şamlar and Hacımaşlı sections, the age of the Soğucak Formation is early Priabonian (SBZ18A-B; Less, Özcan & Okay, 2011). On the Çatalca ridge the phyllites of the Strandja Massif are unconformably overlain by middle–late Priabonian (SBZ19–20) shallow-marine limestones (Fig. 4a; Çatalca-A and B sections of Less, Özcan & Okay, 2011). On the Karaburun peninsula on the Black Sea coast, the Soğukçam Formation is late Priabonian (SBZ20, Figs 5c, d, 7; Less, Özcan & Okay 2011; this study).

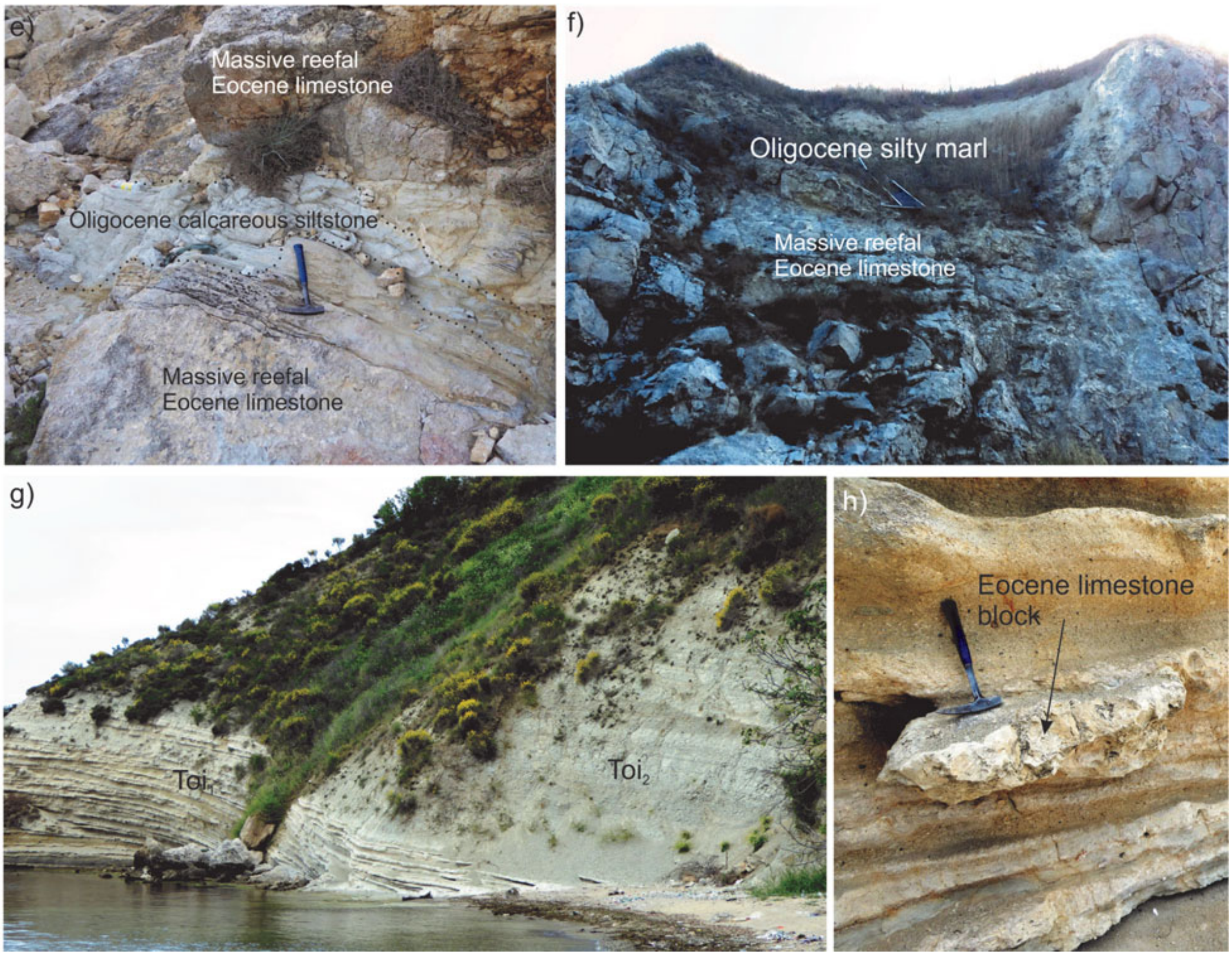

Figure 4. (Colour online) Continued

3.b. Upper Eocene – lower Oligocene pelagic marls and tuffs: the İhsaniye Formation

The Upper Eocene Soğucak Formation is overlain by two distinct sequences in the Çatalca gap. These are a brackish to lagoonal sequence of lower Oligocene sandy limestone and shale, the Pınarhisar Formation, which crops out close to the Çatalca ridge, and the upper Eocene – lower Oligocene pelagic marls of the İhsaniye Formation, which constitute most of the surface geology of the Çatalca gap (Fig. 2).

The İhsaniye Formation consists of light-grey, bluish-grey, beige massive marl, carbonate-rich mudstone interbedded with white limestone and white tuff layers; there are also rare sandstone and conglomerate beds. The tuffs and limestone constitute *c.* 5 % and 7 % of the sequence, respectively, the rest being largely marl. The tuff beds are generally 10–30 cm thick, pure white and consist of very fine-grained, angular quartz, feldspar and rare biotite shards in a glassy matrix; the volcanic glass makes up more than 95 % of the rock and has altered to a mixture of smectite and illite, as shown by the x-ray diffraction (XRD) spectra. The fine, homogeneous grain size and bedded nature of the tuffs indicate that they are ash falls. They must have been the products of volcanic activity in the western part of the Thrace Basin and the Rhodope Massif, where lower Oligocene magmatic rocks are widespread (Eleftheriadis & Lippold, 1984; Ercan *et al.* 1998). The limestones beds are up to 1 m thick and are calc-arenitic. They consist of transported clasts of algae and benthic foraminifera, and are interpreted as calciturbidites. The İhsaniye Formation is poorly consolidated and the bedding is generally subhorizontal. Minimum thickness is 160 m as shown by the Çatalca station well (Erentöz, 1949), and the likely thickness is 300 m.

Planktonic and benthic foraminifera of the İhsaniye Formation were studied in several measured stratigraphic sections (Figs 6, 7). The marls of the İhsaniye Formation contain a rich, well-preserved diverse fauna of planktonic foraminifera. Several tuff horizons from the İhsaniye Formation were also dated using the zircon U–Pb method.

Biostratigraphic data indicate that the base of the İhsaniye Formation is time transgressive and ranges from late Priabonian to early Rupelian in age (planktonic foraminifera zones P16-17 to P19) with the earliest ages recorded in the centre of the Çatalca gap (Fig. 8). In the Sazlıbosna section, shallow-marine sandy limestones of Bartonian–Priabonian transition age (SBZ18A) are overlain by white marl and silty

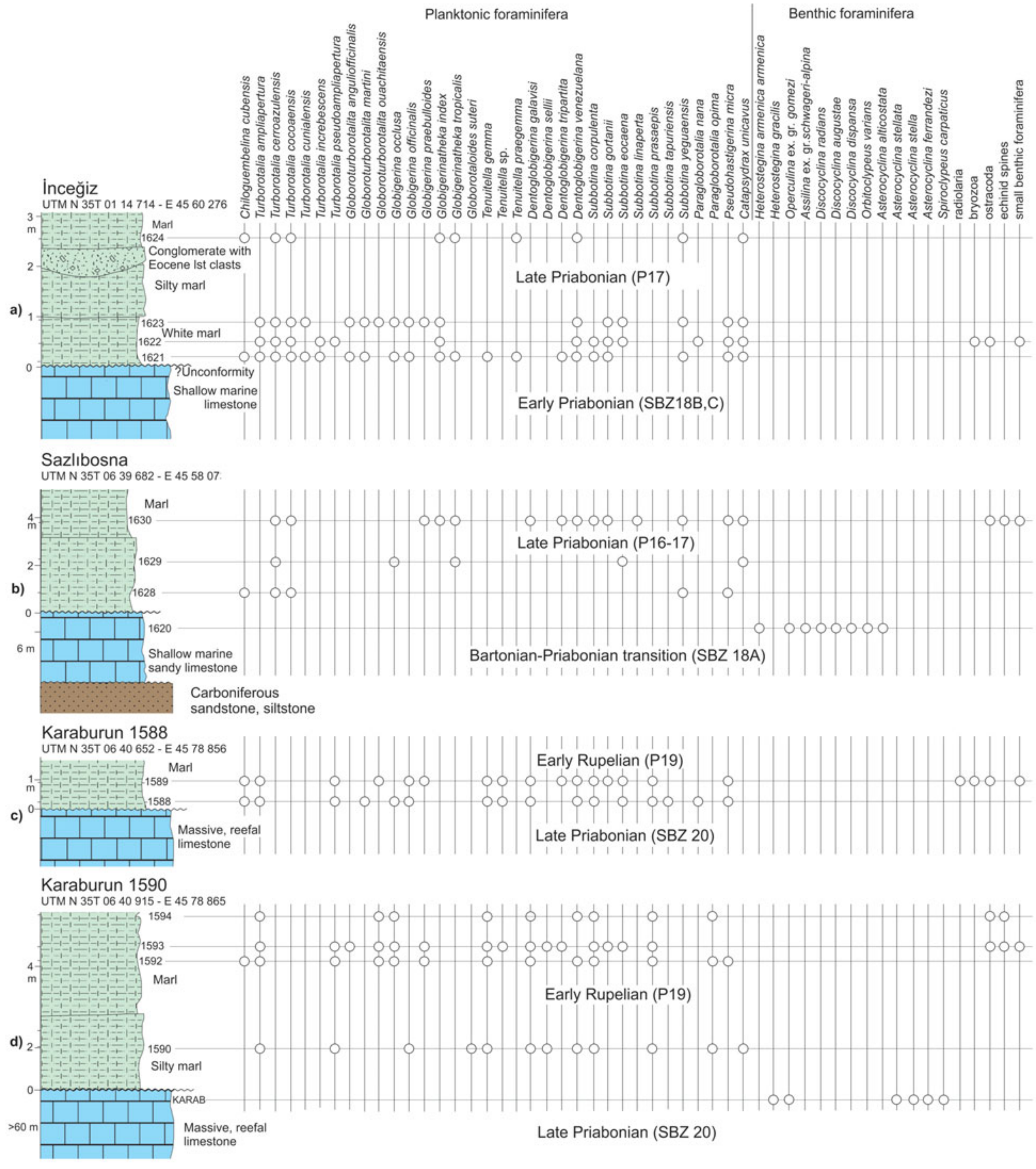

Figure 5. (Colour online) Eocene–Oligocene measured stratigraphic sections in the Çatalca gap and the distribution of the pelagic and benthic foraminifera. For location of the sections see Figure 2.

marl of the İhsaniye Formation, which have yielded late Priabonian (P16-17 zones) planktonic foraminifera (Figs 5b, 7). In the İnceğiz region north of the Çatalca ridge, a 6 m deep channel in the lower Priabonian (SBZ18) shallow-marine limestones of the Soğucak Formation is filled by upper Priabonian (P17 Zone) marl, silty marl and conglomerate with well-rounded clasts of the Soğucak Formation (Fig. 5a). The presence of rounded and lithified clasts of the Soğucak Formation in the upper Eocene marls implies a period of emergence following the deposition of the Soğucak Formation in the İnceğiz region. This unconformity is well exposed in the Karaburun on the Black Sea coast, described in the following section.

3.b.1. *Karaburun on the Black Sea coast*

The Karaburun region is the only known locality along the Thracian Black Sea coast where both Eocene and Oligocene successions are well exposed in 50 m high cliffs. The stratigraphy of the Karaburun region is described by Oktay, Eren & Sakınç (1992), Sakınç (1994)

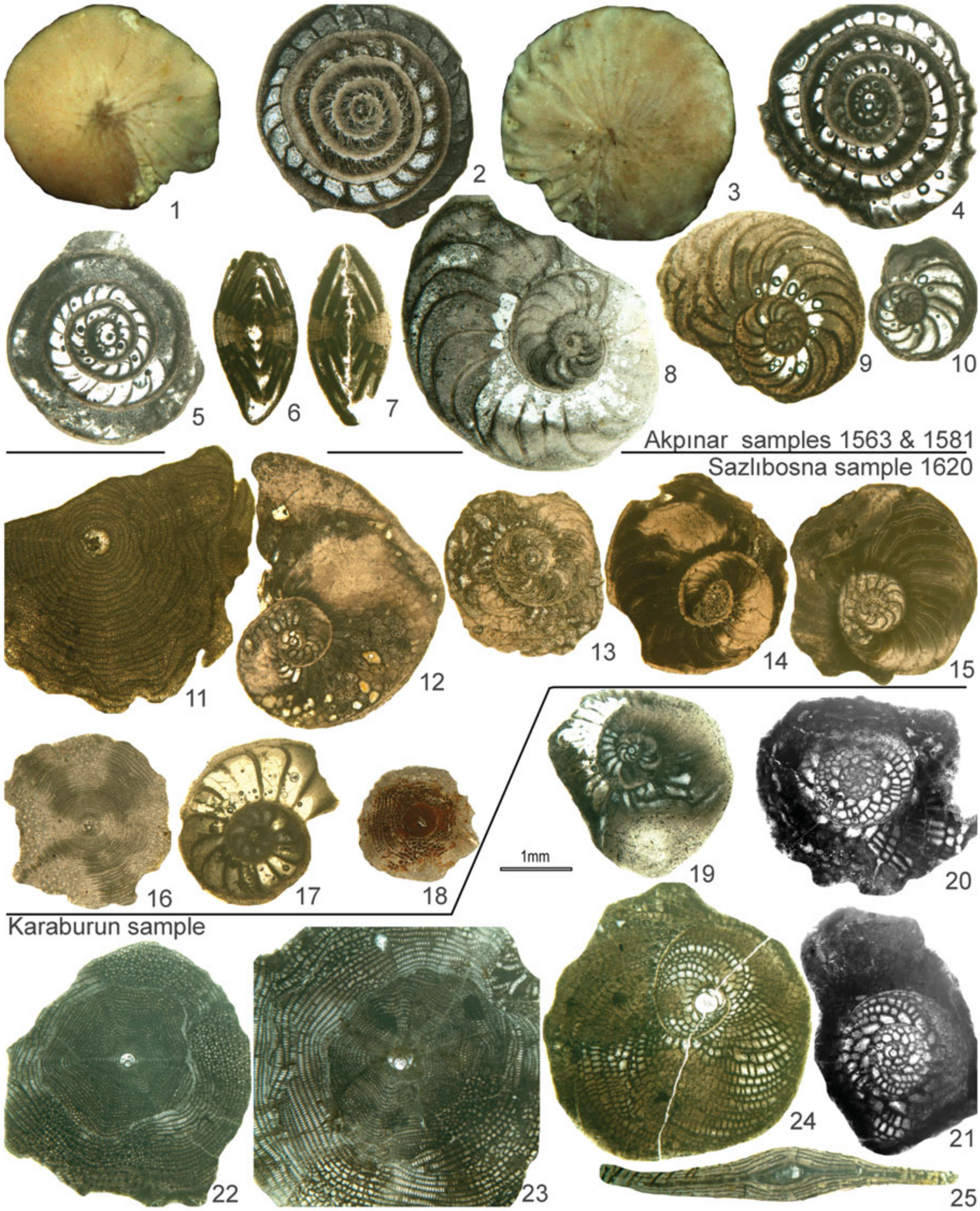

Figure 6. (Colour online) Photographs of large benthic foraminifera from the Soğucak (upper Eocene, 19–25) and İhsaniye (lower Oligocene, 1–18) formations. Akpınar section (Rupelian SBZ 21, cf. Fig. 10). (1–7) *Nummulites vascus* Joly & Leymerie; (1, 2) sample 1581-17; (3, 4) sample 1581-12; (5) sample 1581-18; (6) sample 1563-7; (7) sample 1563-6. (8–10) *Operculina complanata* Defrance; (8) sample 1581–6; (9) sample 1563–8; (10) sample 1563-3. Sazlıbosna section (Bartonian–Priabonian transition, SBZ18A, cf. Fig. 5). (11) *Discocyclina radians* (d'Archiac); sample 1620-1. (12, 13) *Heterostegina armenica armenica* (Grigoryan); (12) sample 1620-12; (13) sample 1620-24. (14, 15) *Operculina* ex. gr. *gomezi* (Colom & Bauza); (14) sample 1620-10; (15) sample 1620–2. (16) *Discocyclina augustae* van der Weijden; sample 1620-11. (17) *Assilina* ex. gr. *schwageri-alpina* (Douville), sample 1620-20. (18) *Orbitoclypeus varians* (Kaufmann), sample 1620–23. Karaburun section (late Priabonian SBZ20). (19) Sample KARAB-6A. (20, 21) *Spiroclypeus carpaticus* (Uhlig); (20) sample KARAB-13; (21) sample KARAB-14. (22) *Asterocyclina stella* (Gümbel), sample KARAB-5A. (24, 25) *Heterostegina gracilis* Herb; (24) sample KARAB-8; (25) KARAB-30. (1, 3) external view; (6–7, 25) axial sections; (11, 16, 18, 22–23) sections along the equatorial layer; others: equatorial sections.

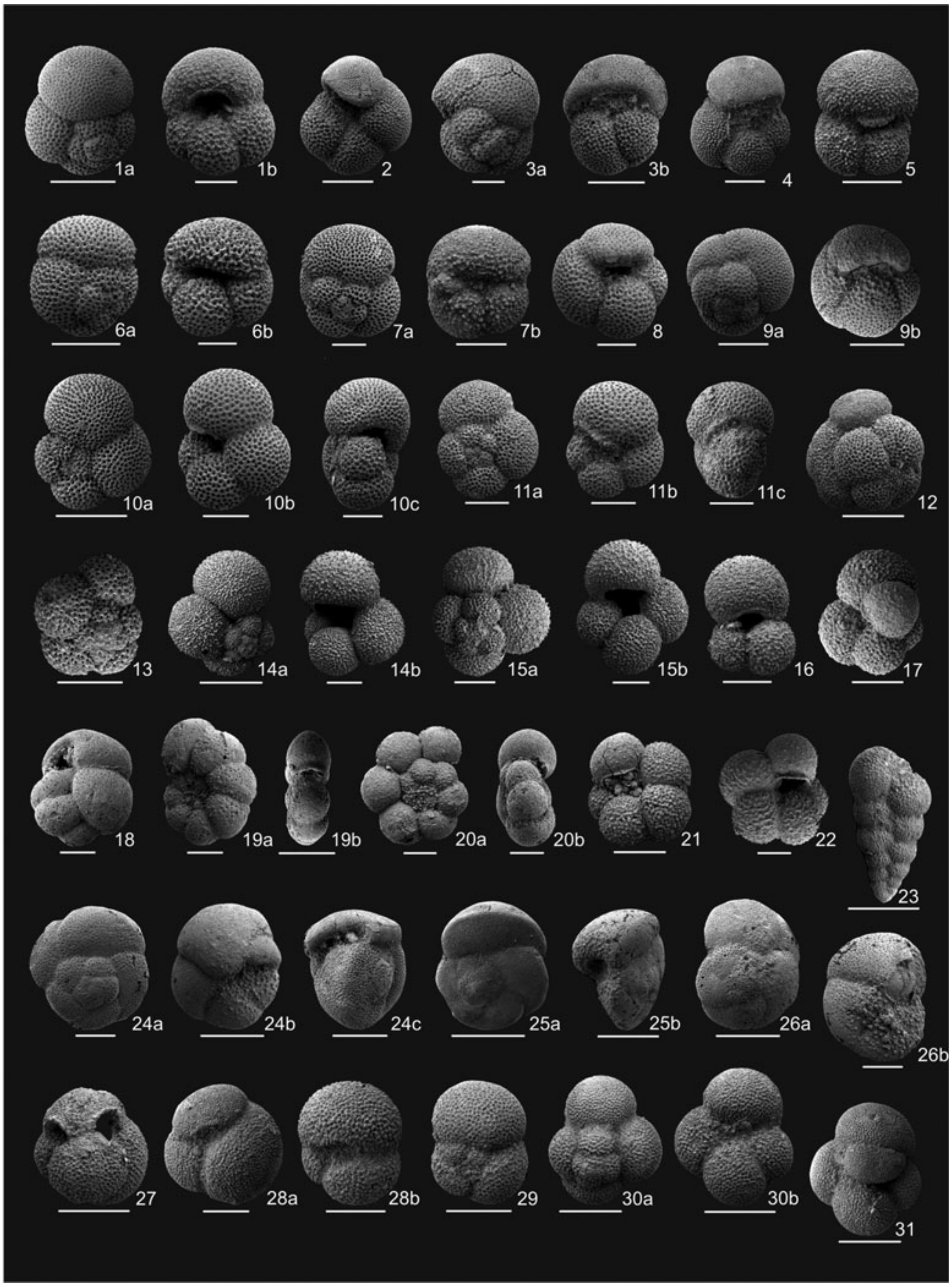

Figure 7. Electron microscope images of planktonic foraminifera from the upper Eocene – lower Oligocene İhsaniye Formation. (1) *Turborotalia ampliapertura* (Bolli): (a) spiral view (200 µm), Kızılcaali sample 1617; (b) umbilical view (100 µm), Kızılcaali 1618; (2) *Turborotalia increbescens* (Bandy), umbilical view (200 µm), Kızılcaali 1607; (3) *Dentoglobigerina sellii* (Borsetti): (a) spiral view (100 µm), Akpınar 1574; (b) umbilical view (200 µm), Kızılcaali 1612; (4) *Turborotalia pseudoampliapertura* (Blow & Banner), umbilical view (200 µm), Kızılcaali 1612; (5) *Dentoglobigerina galavisi* (Bermudez), umbilical view (200 µm), Sazlıbosna 1630; (6) *Globoroturborotalita euapertura* (Jenkins), Akpınar 1573: (a) spiral view (200 µm); (b) umbilical view (100 µm); (7) *Dentoglobigerina tripartita* (Koch): (a) spiral view (100 µm), Kızılcaali 1617; (b) umbilical view (200 µm), Akpınar 1574; (8) *Dentoglobigerina venezuelana* (Hedberg), umbilical view (100 µm), Kızılcaali 1618; (9) *Dentoglobigerina rohri* (Bolli), Kızılcaali 1615: (a) spiral view (200 µm); (b) umbilical view (200 µm); (10) *Paragloborotalia opima* (Bolli): (a) spiral view (200 µm), Akpınar 1576; (b) umbilical view (100 µm), Kızılcaali 1617; (c) side view (100 µm), Akpınar 1576; (11) *Paragloborotalia nana* (Bolli), Akpınar 1576: (a) spiral view (100 µm); (b) umbilical view (100 µm); (c) side view (100 µm); (12) *Subbotina gortanii* (Borsetti), spiral view (300 µm), Kızılcaali 1618; (13) *Globoroturborotalita anguliofficinalis* (Blow), spiral view (100 µm), Akpınar 1576; (14) *Globigerina praebulloides* Blow, Akpınar 1576: (a) spiral view (200 µm); (b) umbilical view (100 µm); (15) *Globigerina occlusa* Blow & Banner: (a) spiral view (100 µm), Kızılcaali 1616; (b) umbilical view (100 µm), Akpınar 1576; (16) *Globigerina leroyi* Blow & Banner, umbilical view (100 µm), Akpınar 1576; (17) *Globoroturborotalita martini* (Blow & Banner), umbilical view (100 µm), Kızılcaali 1618; (18) *Cassigerinella chipolensis* (Cushman & Ponton) (50 µm), Kızılcaali 1618; (19) *Pseudohastigerina micra* (Cole): (a) planispiral view (50 µm), Kızılcaali 1617; (b) side view (100 µm), Akpınar 1561B; (20) *Tenuitella gemma* (Jenkins): (a) spiral view (50 µm), Akpınar 1561B; (b) side view (50 µm), Kızılcaali 1612; (21) *Globigerina ciperoensis* Bolli, umbilical view (100<5.µm), Akpınar 1566; (22)*Tenuitellinata angustiumbilicata* (Bolli), umbilical view (50 µm), Akpınar 1576; (23) *Chiloguembelina cubensis*

and Less, Özcan & Okay (2011). Recently Natal'in & Say (2015) published a completely different stratigraphy for the Eocene–Oligocene succession at Karaburun, which is incompatible with the field data and with the earlier studies as discussed below.

A detailed geological map and cross-section of the region is shown in Figure 9. Massive Eocene reefal limestones with a minimum thickness of 60 m, containing *in situ* corals, algae and benthic foraminifera crop out on the Cape of Karaburun; foraminifera from the upper part of the limestones includes *Spiroclypeus carpaticus*, *Asterocyclina stella* and *Heterostegina gracilis* and indicate a late Priabonian age (SBZ20, Fig. 6). The base of the Soğucak Formation is not exposed but the limestones probably lie above the Upper Cretaceous volcanic rocks, which crop out further east along the coast (Fig. 2).

The Soğucak Formation is unconformably overlain by the marls of the İhsaniye Formation (Oktay, Eren & Sakınç, 1992; Sakınç 1994; Less, Özcan & Okay, 2011). The unconformity surface is marked by patches of dark brown hard ground (Fig. 4d). Further evidence for the unconformity is the presence of Neptunian dykes of the İhsaniye Formation, which extend several metres below the unconformity surface inside the Eocene limestones (Fig. 4e). The Oligocene succession above the Soğucak Formation also includes blocks, up to 1 m large, derived from the Soğucak Formation (Fig. 4h). Natal'in & Say (2015) argue for a conformable contact between the Eocene and Oligocene successions in Karaburun; however, the Eocene limestone shown above the hard ground in figure 4d of Natal'in & Say (2015) as evidence for a conformable contact is not *in situ*.

Two short stratigraphic sections were measured in Karaburun straddling the Eocene–Oligocene boundary (Figs 4d, f, 5c, d). In these sections the massive limestones are overlain by white silty marl; planktonic foraminifera from the marls indicate an early Rupelian age (P19 Zone, Fig. 7) constraining the unconformity to around the Eocene–Oligocene boundary.

The Oligocene succession west of Cape Karaburun is *c.* 100 m thick and can be subdivided into three series (Fig. 9). The lower series, 25 m thick, includes the basal silty marls and an overlying succession of medium-bedded, pebbly calcareous sandstone, siltstone, conglomerate and calc-arenite. The clasts in the calcareous sandstones are mainly rounded, black, grey, dark-green basaltic andesite and andesite with minor Eocene limestone. The volcanic clasts range from sand-sized up to 30 cm across, and in a few beds the clasts are dense enough to call the rock a conglomerate. Eocene limestone clasts are less common but may reach up to 1 m in size (Fig. 4h). The sandstones consist of carbonate and lithic grains with an abundance of bioclastic components. Some beds are rich in *Nummulites vascus*, a lower Oligocene Nummulite species (Sakınç, 1994). The depositional environment is shallow marine, possible a carbonate shore or inner shelf, as suggested by the presence of intact Ostrea (Oktay, Eren & Sakınç, 1992).

The middle part of the Oligocene succession, about 60 m thick, consists principally of an intercalation of light grey marl (about 65 %) and medium-bedded carbonate-rich siltstone and sandstone (30–35 %) with minor debris-flow horizons (Fig. 4g). The marls contain a rich planktonic foraminifer fauna indicating an early Oligocene age (Oktay, Eren & Sakınç, 1992; Gedik *et al.* 2014). The siltstones and sandstones consist principally of carbonate grains with a minor admixture of volcanic clasts and show graded bedding, scoured basal contacts and parallel lamination indicating deposition by turbidite currents. The debris-flow horizons have a channelized geometry with thickness of up to 5 m and are principally composed of Eocene limestone clasts. They increase in intensity upwards in the sequence, and the top 20 m of the Karaburun Oligocene succession is mainly made up of breccia and conglomerate intercalated with disrupted marl horizons. In this part there is also ample evidence for submarine sliding.

3.b.2. *Oligocene sequence in the Çatalca gap*

We measured two stratigraphic sections in the İhsaniye Formation to constrain its age and facies in the centre of the Çatalca gap. The Kızılcaali section is a 125 m thick road section, and the 70 m thick Akpınar section was measured in a civil construction site (Fig. 2). Both sections consist of white, grey homogeneous marl horizons, several metres thick, which are intercalated with thin calc-arenite, argillaceous limestone and acidic tuff beds (Figs 10, 11). There are also rare up to 15 m thick massive channelized limestone breccia horizons representing submarine channels. In the Akpınar section there are occasional beds of brown Mn-rich sandstone, which correlate with the sedimentary manganese deposits of the Pınarhisar Formation close to the Çatalca ridge. Forty-six samples from both sections were studied for foraminifera. The marls are rich in pelagic foraminifera as well in radiolaria, sponge spicules and echinoid fragments (Fig. 7). Planktonic foraminifera

(Palmer) (100 μm), Akpınar 1574; (24) *Turborotalia cerroazulensis* (Cole), İnceğiz 1621: (a) spiral view (200 μm); (b) umbilical view (100 μm); (c) side view (200 μm); (25) *Turborotalia cocoaensis* (Cushman), İnceğiz 1621: (a) spiral view (300 μm); (b) oblique view (200 μm); (26) *Turborotalia cunialensis* (Toumarkine & Bolli), İnceğiz 1621: (a) spiral view (200 μm); (b) side view (100 μm); (27) *Globigerinatheka tropicalis* (Blow & Banner) (200 μm), Sazlıbosna 1630; (28a, b) *Globigerinatheka index* (Finlay), İnceğiz 1621 (100 μm); (29) *Subbotina tapuriensis* (Blow & Banner), spiral view (200 μm), Akpınar 1573; (30) *Subbotina eocaena* (Gümbel): (a) spiral view (300 μm), Akpınar 1567; (b) umbilical view (300 μm), İnceğiz 1621; (31) *Subbotina corpulenta* (Subbotina), umbilical view (300 μm), İnceğiz 1621.

 https://doi.org/10.1017/S0016756817000772

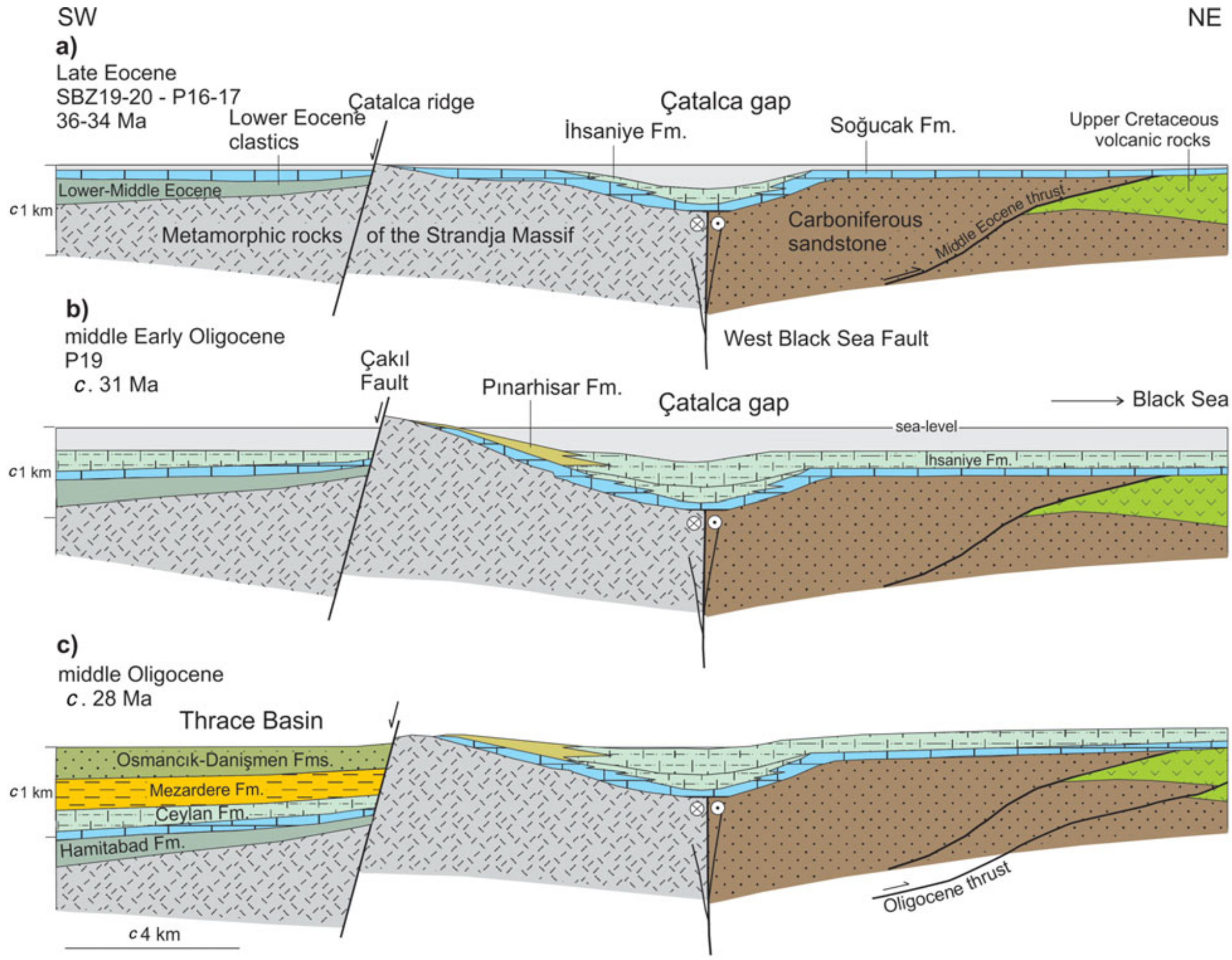

Figure 8. (Colour online) Palaeogeographic cross-sections of the Çatalca gap and the Thrace Basin during late Eocene – middle Oligocene time. The section approximately follows the line of cross-section in Figure 2. (a) During late Eocene time, shallow-marine carbonate deposition characterizes the whole region except the Çatalca gap where pelagic marls are deposited. The Çakıl Fault becomes active at the end of Eocene time. (b) During early Oligocene time, the Çatalca ridge becomes a prominent topographic feature as a result of activity along the Çakıl fault. It controls the sedimentation and separates the Thrace Basin from the Black Sea area. Pelagic marl deposition in the Çatalca gap extends throughout the region except along the Çatalca ridge, where marginal marine to lagoonal limestones and shales, the Pınarhisar Formation, are deposited. (c) The Çakıl Fault continues its activity later during early Oligocene time, creating accommodation space in the Thrace Basin filled by the sandstones of the Osmancık–Danışmen formations. The Çatalca gap becomes an area of non-deposition due to thrusting along the Black Sea margin.

indicate P19 Zone for both sections, corresponding to middle lower Oligocene strata. In the Kızılcaali section the presence of *Pseudohastigerina micra* in all samples and the regular appearance of *Paragloborotalia opima* above sample 1615 suggest that the section represents the lower and middle part of the P19 Zone (Coccioni *et al*. 2008). In the Akpınar section the absence of *Pseudohastigerina micra* (except for in the basal sample) and abundance of *Paragloborotalia opima* indicate that that section represents the upper part of the P19 Zone. Both sections contain transported benthic foraminifera, which indicate a broad early Oligocene age (Fig. 6).

There are two white tuff horizons in the Akpınar section (Fig. 10). Zircons from these tuff horizons were dated in UC Santa Barbara using LA-ICP-MS. A sample from the upper tuff bed (1586) gave a precise U–Pb age of 31.05 ± 0.19 Ma (0.62) (Fig. 12a; Supplementary Table S1). Zircons from the lower horizon show a scattered age population; however three zircons indicate an age of 32.3 ± 1.8 Ma (Fig. 12b; Supplementary Table S2). In the Kızılcaali section there are five tuff beds; the topmost tuff bed yielded a precise zircon U–Pb age of 31.51 ± 0.91 Ma (Fig. 12c; Supplementary Table S3). These zircon ages are compatible with the biostratigraphic data and indicate a middle early Oligocene (P19 Zone) age for the Akpınar and Kızılcaali sections. A spot tuff sample from the İhsaniye Formation collected from north of Çatalca (sample 1560 in Fig. 2) produced a similar zircon U–Pb age of 31.63 ± 0.31 (0.63) Ma (Fig. 12d; Supplementary Table S4). Biostratigraphic data and zircon U–Pb ages therefore indicate a middle early Oligocene age for the İhsaniye Formation. The

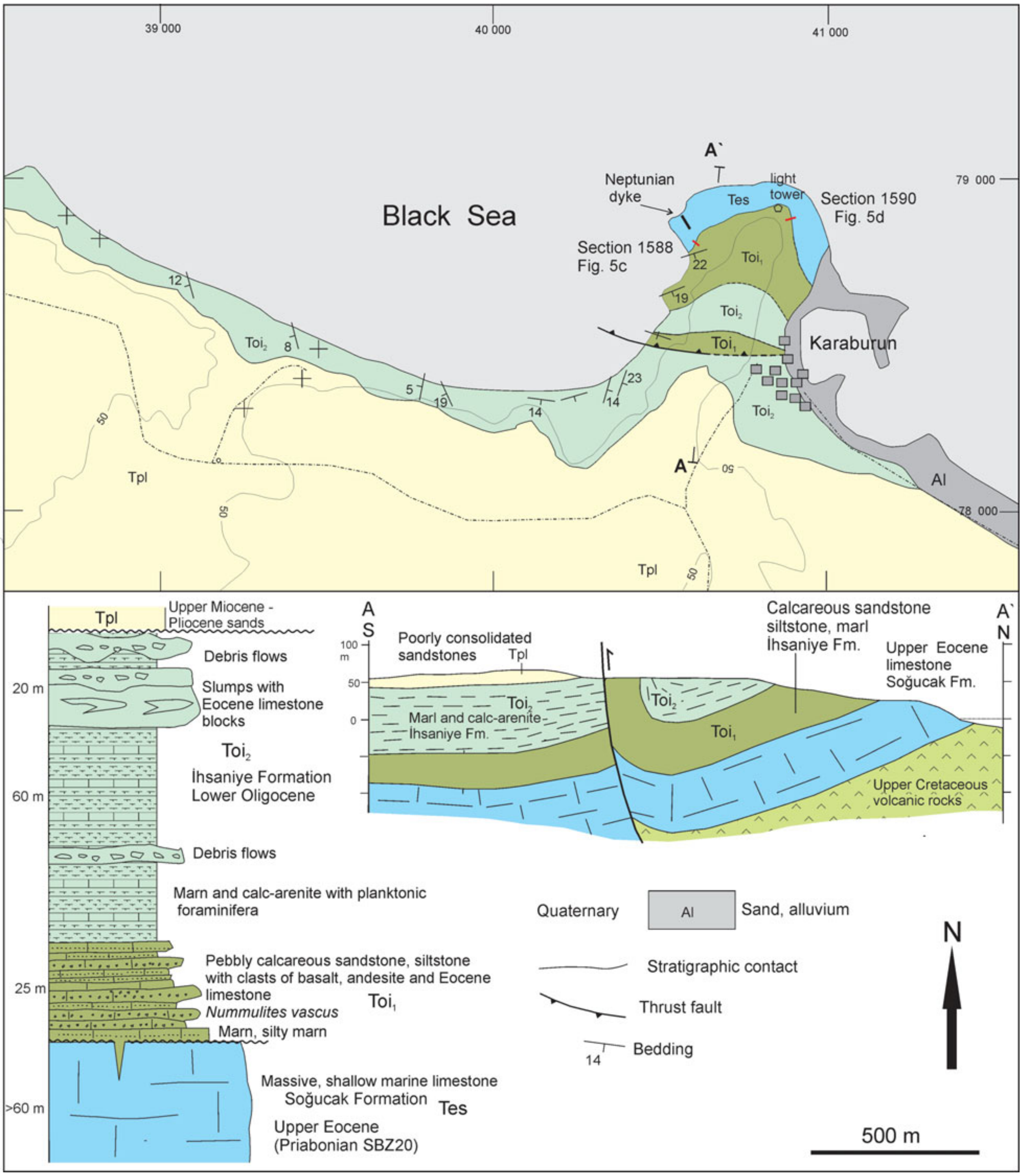

Figure 9. (Colour online) Geological map, cross-section and stratigraphic section of the Karaburun region. For location see Figure 2. The coordinates are in UTM in European 1979 datum.

presence of pelagic foraminifera, radiolaria and channelized debris flows indicate a deep outer shelf for its depositional environment.

In the Çatalca gap the İhsaniye Formation is unconformably overlain by Miocene fluviatile and limnic sedimentary rocks (Figs 2, 3; Suc *et al.* 2015). The subhorizontal bedding and general absence of shortening structures in the İhsaniye Formation and lack of any evidence for shallowing upwards suggest that the uplift of the Çatalca gap occurred during early Oligocene time along deep-seated faults on the Black Sea margin. An example of such a reverse fault is observed in Karaburun (Fig. 9; Oktay, Eren & Sakınç, 1992; Natal'in & Say, 2015). In contrast to the Çatalca gap, the sedimentary sequence in the Thrace Basin west of the Çatalca ridge is much thicker and continues into upper Oligocene strata (Fig. 8). Similarly, seismic reflection sections in the West Black Sea Basin suggest that the Oligocene – lower Miocene Maykop sequence is several kilometres thick (Nikishin *et al.* 2015*a*).

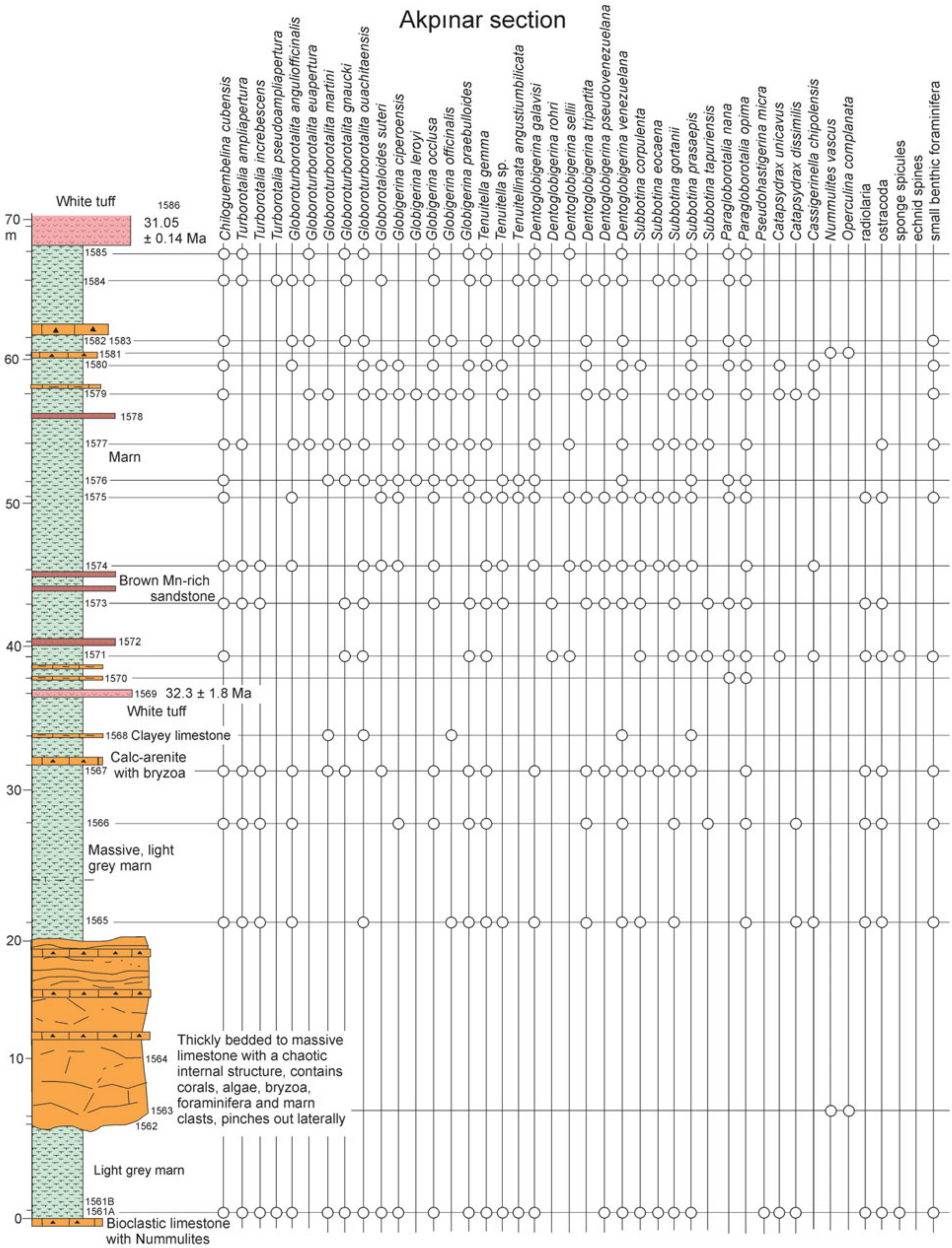

Figure 10. (Colour online) Akpınar measured stratigraphic section in the lower Oligocene İhsaniye Formation and the distribution of pelagic foraminifera. For location of the sections see Figure 2.

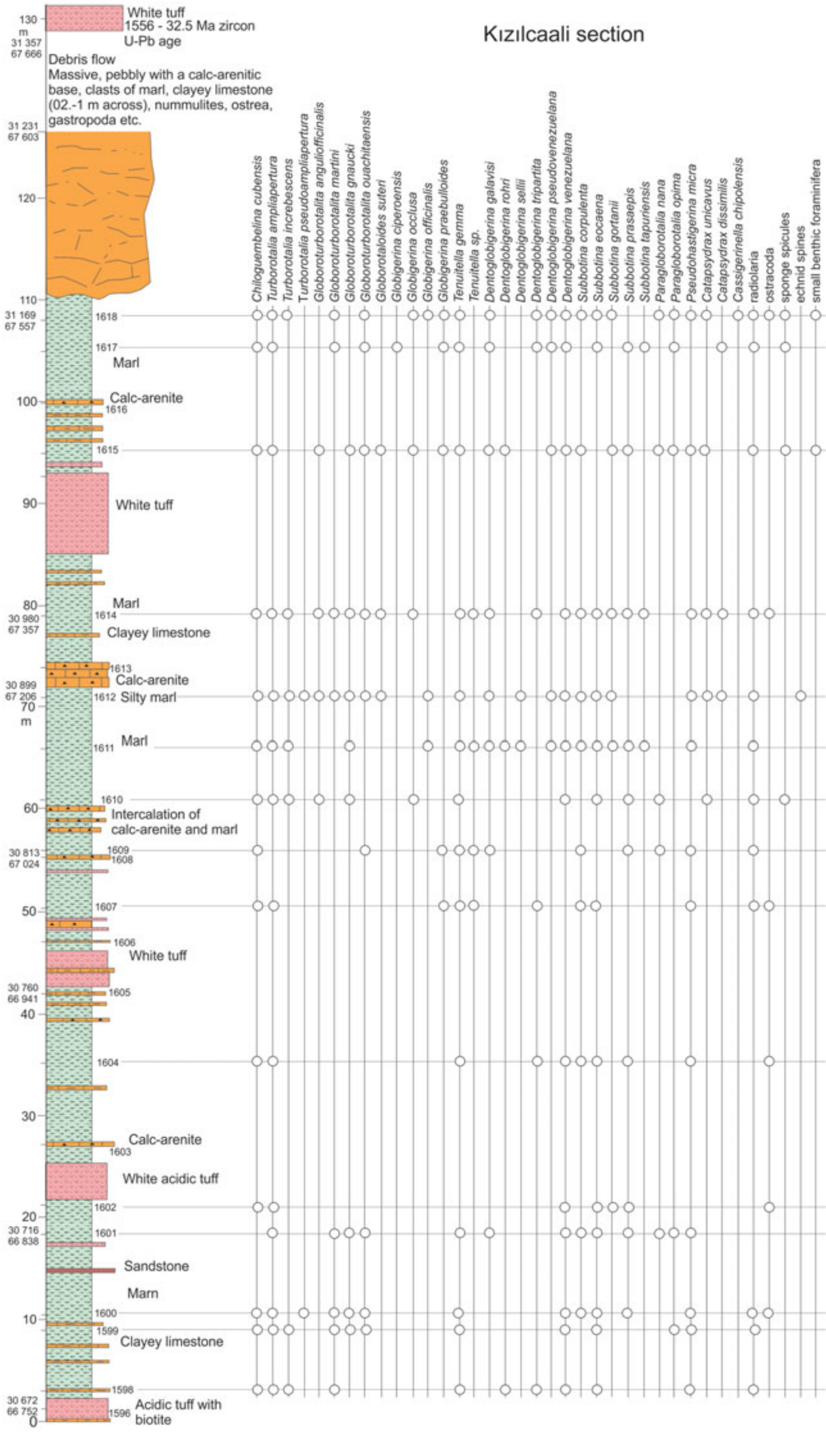

Figure 11. (Colour online) Kızılcaali measured stratigraphic section in the lower Oligocene İhsaniye Formation and the distribution of pelagic foraminifera. For location of the sections see Figure 2.

3.c. Oligocene sandy limestone, manganese deposits and dark shales: the Pınarhisar Formation

In the vicinity of the Çatalca ridge, the lower Oligocene sequence consists of lagoonal porous pebbly, sandy limestone, conglomerate and shale, called the Pınarhisar Formation (Fig. 13; Akartuna, 1953; Gökçen, 1973). The sequence crops out on the northeastern margin of the Çatalca ridge, where it lies above the upper Eocene limestones with an angular unconformity (Fig. 4c). The sandy limestones contain an abundance of the brackish bivalves, and are overlain by dark laminated shales with fish fossils and plant remains (Akartuna, 1953; Gökçen, 1973). Similar Oligocene lagoonal sequences crop out further NW on the margins of the Thrace Basin (İslamoğlu *et al.* 2008).

In the Çatalca region sedimentary manganese deposits consisting of pisolithic manganese ore occur locally at the contact between the lagoonal limestones and shales (Fig. 13; Gültekin, 1998). Lower Oligocene

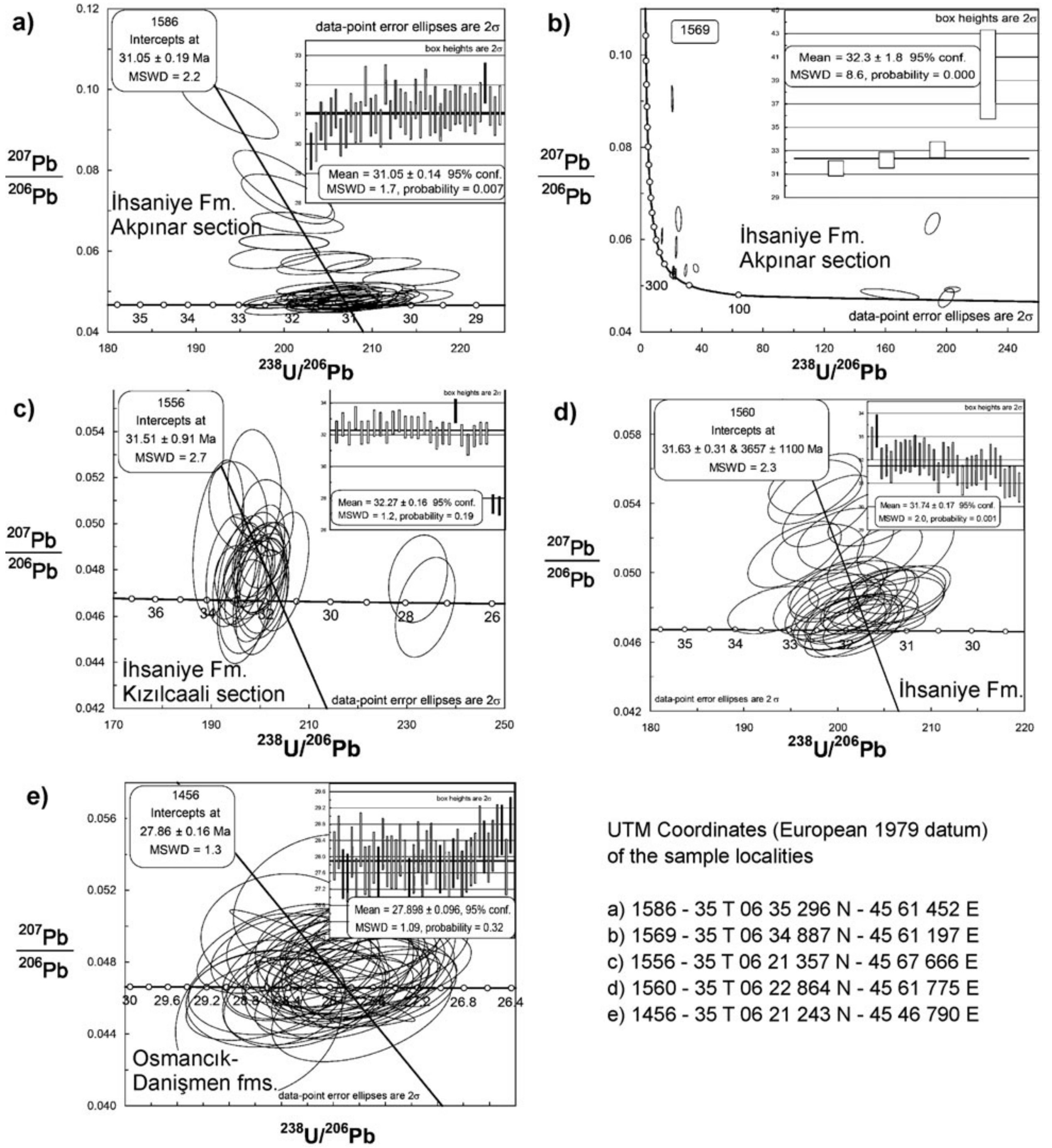

Figure 12. Zircon U–Pb diagrams for the acidic tuffs from (a–d) the İhsaniye Formation and (e) the Osmancık–Danişment formations. For analytical data see Supplementary Tables S1–S5.

manganese deposits are common in the Paratethys and have been described from the Balkans, Georgia and Russia (Öztürk & Frakes, 1995; Varentsov, 2002) but are unknown from the Tethyan realm (cf. İslamoğlu *et al.* 2008). They formed during a unique depositional event (Solenovian event) during early Oligocene time, dated to NP22–23 (NP: nannoplankton; *c.* 32 Ma; Soták *et al.* 2001; Rojkovič *et al.* 2008; Sachsenhofer *et al*. 2009). The rare Mn-rich sandstone beds in the İhsaniye Formation represent a distant reflection of this event. An early Oligocene age for the Pınarhisar Formation is also indicated by its ostracod fauna (Gökçen, 1973). The Pınarhisar Formation is therefore coeval with the İhsaniye Formation, but represents a lagoonal and restricted marine environment closer to the land (Fig. 8).

4. The Çatalca ridge and the Thrace Basin

The Çatalca ridge constitutes the boundary between the Çatalca gap and the Thrace Basin (Fig. 2). It forms a narrow horst, bounded by two subparallel normal faults (Fig. 13). The main fault with 2 km of vertical total offset, the Çakıl Fault, is on the southwestern side

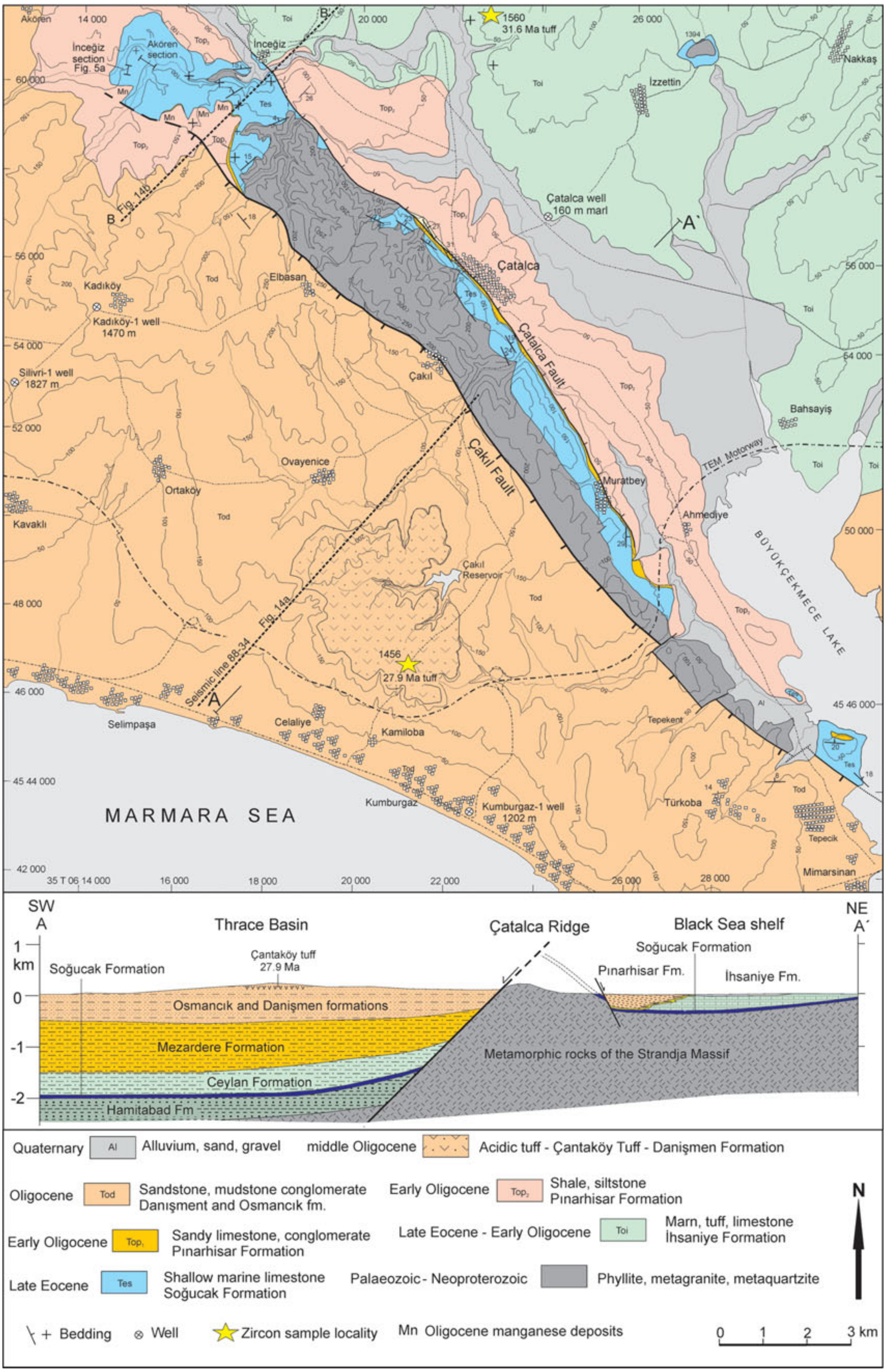

Figure 13. (Colour online) Geological map and cross-section of the Çatalca region (based on Akartuna, 1953; Gedik *et al.* 2014; and our mapping). The coordinates are in UTM in European 1979 datum.

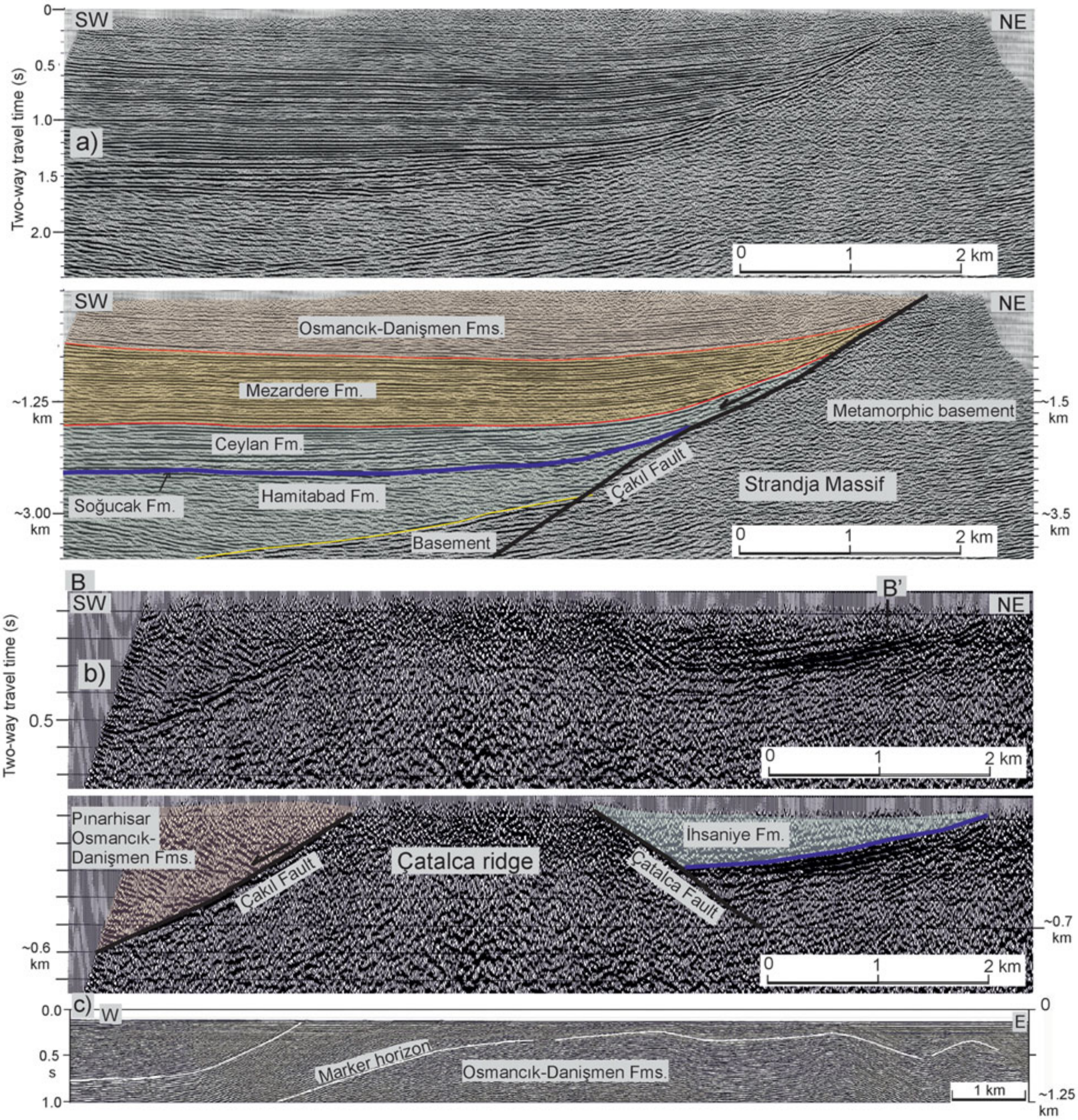

Figure 14. (Colour online) Time-migrated seismic reflection sections of lines (a) 88-34 and (b) MAD-90-311 perpendicular to the Çatalca ridge and (c) MCS02 in the Marmara Sea. For the location of the profile see Figures 2 and 13. Line MCS02 is modified from Ergintav *et al*. (2011).

of the ridge; the morphologically more distinct Çatalca fault on the northeastern side has a smaller total vertical slip of *c*. 300 m (Fig. 14). The relatively minor offset along the Çatalca Fault is also evident from the observation that the metamorphic basement crops out seven kilometres NE of Çatalca ridge (Fig. 13).

A seismic reflection section perpendicular to the Çakıl Fault shows it to be a planar fault dipping at *c*. 45° (Fig. 14a). A magnetotelluric profile across the Çakıl Fault also shows it to be a SW-dipping major structure (Karcıoğlu *et al*. 2013). The Çakıl Fault is one of several en échelon normal faults forming the northeastern boundary of the Thrace Basin. The other faults are buried by the upper Miocene strata and are only recognized in the seismic sections (Turgut, Türkarslan & Perinçek, 1991; Perinçek, 1991); Çakıl Fault is unique in juxtaposing metamorphic rocks of the Strandja Massif against the Oligocene sandstones in outcrop (Fig. 13).

The Thrace Basins sequence west of the Çatalca ridge is principally known from the wells and seismic sections. These show the presence of a >2 km thick clastic-dominated Eocene–Oligocene succession, which contrasts with the 300 m thick Eocene–Oligocene succession in the Çatalca gap (Fig. 13). At the base lies the 400 m thick lower–middle Eocene succession, the Hamitabad Formation, which is not present in the Çatalca gap (Figs 14a, 15). The

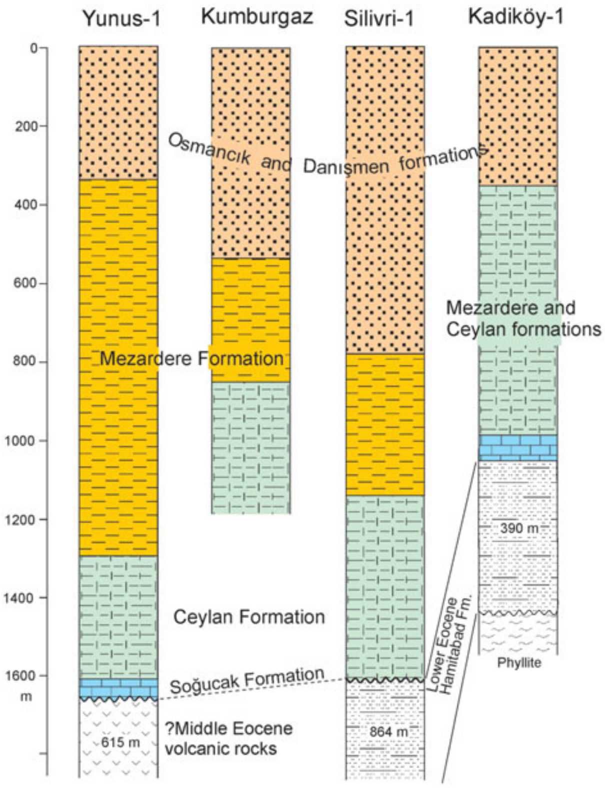

Figure 15. (Colour online) Simplified lithological logs for some of the wells in Thrace Basin west of the Çatalca ridge (Turgut & Eseller, 2000; Hoşgörmez & Yalçın, 2005). For the location of the wells see Figures 2 and 13.

Hamitabad Formation in the Thrace Basin is principally known from wells and seismic sections; it encompasses a variety of clastic facies from turbidites to continental clastic rocks (Turgut, Türkarslan & Perinçek, 1991; Siyako & Huvaz, 2007). In the seismic sections the top of the Hamitabad Formation is a major unconformity (cf. fig. 7 of Siyako & Huvaz, 2007). Vitrinite reflectance values also exhibit a change above the Hamitabad Formation (Huvaz, Sarikaya & Nohut, 2005). These observations indicate a major break in sedimentation during middle Eocene time, which was a time of contractional deformation, uplift and erosion in the western Anatolia and in the Balkanides (Sinclair *et al.* 1997; Özcan *et al.* 2012). The lower–middle Eocene succession in the Çatalca gap must have been eroded during this contractional episode.

West of the Çatalca ridge the Hamitabad Formation is overlain by shallow-marine limestones of the Soğucak Formation, a few tens of metres thickness, which pass up into shale and marl of the upper Eocene – lower Oligocene Ceylan Formation. The Ceylan Formation occurs widely in the subsurface in the eastern part of the Thrace Basin (Siyako & Huvaz, 2007); it correlates in part with the İhsaniye Formation. The Ceylan Formation is overlain by shale with minor sandstone, the Mezardere Formation, deposited in the slope and frontal plain of a major delta (Turgut, Türkarslan & Perinçek, 1991; Siyako & Huvaz, 2007). The Mezardere Formation passes up into a paralic Oligocene sequence of sandstone, conglomerate and mudstone with lignite seams and tuff horizons, >500 m in thickness, which crops out on the surface (Fig. 13). This sequence represents delta front and delta plain deposits and has been divided into Osmancık and Danişmen formations (Turgut & Eseller, 2000). The division is mainly on the basis of seismic data (e.g. Siyako, 2006); the distinction is difficult to make in outcrop. The Osmancık–Danişmen formations represent the terminal stage of the Thrace Basin (Turgut, Türkarslan & Perinçek, 1991; Siyako, 2006; Siyako & Huvaz, 2007; Perinçek *et al.* 2015). The sandstones of the Osmancık–Danişmen formations dip gently to the SE and cover the southeastern projection of the Çakıl Fault (Fig. 2). This is also illustrated by a seismic reflection profile on the northern margin of the Marmara Sea south of Avcılar, which shows a gently folded Oligocene sequence with no evidence for a major fault (Figs 2, 14c; Ergintav *et al.* 2011). These observations suggest a decrease in activity of the Çakıl Fault towards the end of the deposition of the Osmancık–Danişmen formations during late Oligocene time.

The Osmancık–Danişmen formations are usually assigned a broad Oligocene age (mostly late Rupelian – early Chattian) based on vertebrate faunas and palynomorphs (Ozansoy, 1962; Lebküchner, 1974; Ediger & Alişan, 1989; Ünay-Bayraktar, 1989); however, many studies extend their age into the early Miocene (Turgut, Türkarslan & Perinçek, 1991; Turgut & Eseller, 2000; Siyako, 2006; Perinçek *et al.* 2015). We dated zircons from the tuffs from the uppermost parts of the Osmancık–Danişmen succession to constrain the top age of the Thrace Basin and that of the Çakıl Fault. White porous tuffs, the Çantaköy tuff, constitute the topmost part of the Osmancık–Danişmen formations SW of the Çatalca ridge (Fig. 13). Zircons from a sample (1456) of the Çantaköy tuff gave a middle Oligocene U–Pb age of 27.86 ± 0.16 Ma (0.56) (Fig. 12e; Supplementary Table S5). Zircon U–Pb ages between 25.4 Ma and 24.3 Ma are reported from tuffs in the Osmancık–Danişmen formations from further SE in the Beylikdüzü region (Fig. 2; Arpat, 2017; Timur Ustaömer, pers. comm., 2017). These tuffs lie above the SE projection of the Çakıl and Çatalca faults. These zircon ages indicate that the sedimentation in the Thrace Basin ended during late Oligocene time and the activity of the Çakıl Fault was terminated by middle Oligocene time.

The Eocene shallow-marine limestone of the Soğucak Formation, which is on the surface at 200 m above sea level on the Çatalca ridge, was encountered in the Kadiköy-1 and Yunus-1 wells at depths of 1000 m and 1600 m below the surface, respectively (Fig. 15). In the seismic section the Soğucak Formation is imaged at a two-way travel time of 1.6 s, equivalent to a depth of *c.* 1.8 km, at a distance of 6 km SW of the Çatalca ridge (Fig. 14a). The correlation of the subsurface and surface Soğucak Formation indicates *c.* 2 km of vertical offset along the Çakıl Fault. The subsurface Soğucak Formation is most probably late Eocene in age, the same as that for the Çatalca ridge (SBZ19–20, 37–34 Ma; Less, Özcan & Okay, 2011). This would indicate that the Çakıl Fault was active from late Eocene until middle Oligocene time (37–28 Ma) for a period of *c.* 9 Ma, when it accumulated a vertical offset of *c.* 2 km.

In extensional basins, the syntectonic sediments increase in thickness towards the bounding faults (e.g. Gawthorpe & Leeder, 2000). Although the Çakıl Fault has a large cumulative offset, the seismic section shows no such increase towards the fault (Fig. 14a). This is also the case for the other normal faults along the northeastern margin of the Thrace Basin (cf. Perinçek, 1991; Turgut, Türkarslan & Perinçek, 1991), suggesting that the locus of subsidence in the Thrace Basin was in the centre and not on the marginal faults.

5. Geological evolution

5.a. Early–middle Eocene sedimentation and middle Eocene shortening

During early–middle Eocene time there was widespread siliciclastic turbidite deposition in northern Anatolia (Saner, 1980; Özcan *et al.* 2012); the realm of turbidite deposition included much of the present Thrace Basin and extended to the Black Sea (Fig. 1). There is no evidence that the Thrace Basin existed as a separate depocentre during early Eocene time.

During early middle Eocene time there was a major phase of shortening in the Anatolia and Balkans. The Palaeozoic sequence of the Istanbul region was thrust north over the Upper Cretaceous volcanic rocks (Fig. 1; Baykal, 1943; Baykal & Önalan, 1980). This thrust can be traced for over 50 km on both sides of the Bosphorus (Fig. 2), and is recorded in an intra-Eocene angular unconformity in the Şile region on the Black Sea coast, where lower Lutetian (SBZ13) shallow-marine limestones lie with an angular unconformity over a lower Eocene sequence (Baykal & Önalan, 1980; Özcan, Less & Kertész, 2007; Özgül, 2012). The north-vergent thrusting in the Balkanides also started during middle Eocene time (Sinclair *et al.* 1997) and was widespread in the southern Balkans (Burchfiel *et al.* 2008). An episode of intra-Eocene folding is also observed in the seismic sections in the western Black Sea shelf (Menlikli *et al*. 2009; Georgiev, 2012; Nikishin *et al*. 2015*a*). The widespread contraction and resultant uplift led to the termination of sedimentation and erosion over a large region. In NW Anatolia the marine sedimentation ended during early Lutetian time (*c.* 45 Ma) and the region has been above sea level since then (Özcan *et al.* 2012). The lower Eocene sequence in the Çatalca gap was eroded during middle Eocene time. A remnant early–middle Eocene basin may have survived the middle Eocene deformation in the centre of the Thrace Basin; however, there is no evidence that there was a connection to the West Black Sea Basin during late middle Eocene time.

5.b. Late Eocene transgression in the Thrace Basin

During late Eocene time the western Anatolia and the Aegean region remained as erosional areas. The only exception was the Thrace Basin, where the realm of marine deposition expanded to its present outlines. A connection with the Black Sea was established through the Çatalca gap at the base of the upper Eocene strata (SBZ18A), when shallow-marine limestones were deposited in the centre of the Çatalca gap. The transgression was gradual and the Çatalca ridge was flooded during middle late Eocene time (SBZ19). A second connection between the Thrace Basin and the Black Sea existed during middle late Eocene time through Kıyıköy and Vize (Fig. 1; Less, Özcan & Okay, 2011). Towards the end of late Eocene time, the deposition of pelagic marls expanded from the Black Sea to the Çatalca gap and probably to the Thrace Basin. Upper Eocene marls are also reported fom the onshore and offshore parts of the Burgas Basin in the Black Sea (Fig. 1; Juranov, 1992; Georgiev, 2012).

5.c. Early Oligocene

During early Oligocene time the Kıyıköy–Vize connection was largely terminated and the Çatalca gap was the only connection between the Black Sea and the Thrace Basin. Deep-marine marls were deposited in the Çatalca gap and in the eastern part of the Thrace Basin. Some studies have suggested that clastic turbidites were transported from the Thrace Basin to the West Black Sea during early Oligocene time through the Çatalca gap (e.g. Nikishin *et al*. 2015*b*). However, the Thrace Basin was sourced from the west from the Rhodope Massif and from the south (D'Atri *et al*. 2012; Cavazza *et al.* 2013) and little clastic sediment reached the eastern parts of the Thrace Basin during early Rupelian time. Sedimentation of marls in the Çatalca gap during early Oligocene time also indicates a lack of clastic transport from the Thrace Basin into the Black Sea during this period. The connection to the Black Sea was closed during middle Rupelian time (at the end of the P19 Zone, *c.* 30 Ma) through thrusting and uplift along the Black Sea margin.

The Eocene–Oligocene boundary is usually taken as the time when the Tethys ocean split into a Paratethys in the north and Mediterranean in the south separated by a discontinuous land bridge extending from Iran through Turkey to Central Europe (e.g. Rögl, 1999; Steininger & Wessel, 1999). The lower Oligocene sequence offshore Bulgaria is characterized by anoxic shale and marl (Sachsenhofer *et al*. 2009), whereas the Çatalca gap (and by implication the Thrace Basin), regarded as part of the Paratethys, had fully marine conditions during late Eocene – early Oligocene time with a well-developed marine fauna. The typical Paratethyan facies and faunas, such as those observed in the Pınarhisar Formation (e.g. İslamoğlu *et al.* 2008), were restricted to regions close to land.

In the Thrace Basin there was a change from carbonate to clastic deposition and a drastic increase in the rate of sedimentation durin early Oligocene time. Shallow-marine limestones of the Soğucak Formation have a thickness of 20–80 m, whereas the overlying upper Eocene – middle Oligocene siliciclastic sequence in the Thrace Basin is several kilometres thick (Turgut, Türkarslan & Perinçek, 1991). During middle Rupelian time a major delta propagated from the south and SW into the Thrace Basin, filling it up gradually during middle Oligocene time (Şenol, 1980). The sedimentation in the Thrace Basin ended by late Oligocene time followed by shortening during latest Oligocene – early Miocene time.

6. Conclusions

New biostratigraphic, geochronological and geological data and critical appraisal of published data have lead to a number of conclusions regarding the Thrace Basin and its connection to the West Black Sea Basin.

1. During early and middle Eocene time the Thrace Basin and the Pontides were a realm of clastic deposition, which also encompassed the Black Sea. This depositional period ended with a major phase of contractional deformation during late middle Eocene time in the Pontides with erosion of the lower–middle Eocene sequences over large areas. The Black Sea and a remnant Thrace Basin survived the middle Eocene deformation.

2. A marine connection was established from the Black Sea to the Thrace Basin at the base of the upper Eocene strata through the Çatalca gap west of Istanbul. This led to widespread marine transgression in the Thrace Basin.

3. During late Eocene – early Oligocene time (38–31 Ma), the marine connection with the Black Sea was maintained through the Çatalca gap west of Istanbul. The Çatalca gap follows the damage zone of the Late Cretaceous West Black Sea Fault.

4. Major faults create damage zones, which form axial valleys and may act as marine gateways. The West Black Sea Fault zone acted as such a marine gateway during late Eocene – early Oligocene time between the Black Sea and the Thrace Basin (Fig. 8).

5. The marine gateway between the Black Sea and the Thrace Basin was closed during middle early Oligocene time (*c.* 30 Ma, end of the P19 Zone) through thrusting along the Black Sea margin (Fig. 8). The closure of the marine connection eventually led to the paralic conditions in the Thrace Basin.

6. Although there was a marine connection between the Thrace Basin and the Black Sea during late Eocene – early Oligocene time, there was no exchange of clastic sediment. The sedimentary sequence in the Çatalca gap consists of shallow-marine upper Eocene limestones overlain by lower Oligocene pelagic marls (Fig. 12).

7. The Black Sea and the Thrace Basin are considered as part of the Paratethys during early Oligocene time; however, fully marine sequences with a rich fauna of foraminifera were deposited in both basins during middle early Oligocene time.

Acknowledgements. This study was supported by Istanbul Technical University BAP project No. 34772 and partly by TÜBA. We thank Timur Ustaömer for information on zircon ages, Ömer Işık Ece for XRD work and Emin Demirbağ, Necdet Özgül and Oğuz Göğüş for useful discussions. Constructive and detailed reviews by Namık Çağatay and Georgi Georgiev greatly improved the manuscript.

Supplementary material

To view supplementary material for this article, please visit https://doi.org/10.1017/S0016756817000772

References

Akartuna, M. 1953. *Geology of the Çatalca-Karacaköy Region* (in Turkish). University of Istanbul, Istanbul Üniversitesi Fen Fakültesi Monografileri 13, 88 pp.

Arpat, E. 2017. The sediments of an Early Miocene river system developed from the Marmara Sea area toward the Black Sea. *Proceedings of the 5th Symposium on the Geology of Istanbul*, Istanbul, 12–14 May 2017, 73–83.

Baykal, A. F. 1943. *La Géologie de la Région de Şile (Bithynie-Anatolie)*. University of Istanbul, Istanbul Üniversitesi Fen Fakültesi Monografileri 3, 233 pp.

Baykal, A. F. & Önalan, M. 1980, Şile sedimentary melange (Şile Olistostrome) (in Turkish). *Proceedings of the Altınlı Symposium*, Ankara. Türkiye Jeoloji Kurumu, 15–25.

Berggren, W. A., Kent, D. V., Swisher, C. C. & Aubry, M. P. 1995. A revised Cenozoic geochronology and chronostratigraphy. In *Geochronology, Time Scales and Global Stratigraphic Correlation* (eds W. A. Berggren, D. V. Kent, M. P. Aubry & J. Hardenbol), pp. 129–212. Society of Economic Paleontologists and Mineralogists (SEPM), Special Publication 54.

Burchfiel, B. C., Nakov, R., Dumurdzanov, N., Papanikolaou, D., Tzankov, T., Serafimovski, T., King, R. W., Kotzev, V., Todosov, A. & Nurce, B. 2008. Evolution and dynamics of the Cenozoic tectonics of the South Balkan extensional system. *Geosphere* **4**, 919–38.

Cattò, S., Cavazza, W., Zattin, M. & Okay, A.I. 2017. No significant Alpine-age tectonic overprint of the Cimmerian Strandja Massif (SE Bulgaria and NW Turkey). *International Geology Review*, published online 17 July 2017, doi: 10.1080/00206814.2017.1350604

Cavazza, W., Caracciolo, L., Critelli, S., d'Atri, A. & Zuffaa, G. G. 2013. Petrostratigraphic evolution of the Thrace Basin (Bulgaria, Greece, Turkey) within the context of Eocene-Oligocene post-collisional evolution of the Vardar-İzmir-Ankara suture zone. *Geodinamica Acta* **26**, 27–55.

Coccioni, R., Montanari, A., Bellanca, A., Bice, D. M., Brinkhuis, H., Church, N., Deino, A., Lirer, F., Macalady, A., Maiorano, P., Marsili, A., McDaniel, A., Monechi, S., Neri, R., Nini, C., Nocchi, M., Pross, J., Rochette, P., Sagnotti, L., Sprovieri, M., Tateo, F., Touchard, Y., Van Simaeys, S. & Williams, G. L. 2008. Integrated stratigraphy of the

Oligocene pelagic sequence in the Umbria-Marche basin (Northeastern Apennines, Italy): a potential Global Stratotype Section and Point (GSSP) for the Rupelian/Chattian boundary. *Geological Society of America Bulletin* **120**, 487–511.

Costa, E., Garcés, M., López-Blanco, M., Serra-Kiel, J., Bernaola, G., Cabrera, L. & Beamud, E. 2013. The Bartonian-Priabonian marine record of the eastern South Pyrenean foreland basin (NE Spain): a new calibration of the larger foraminifers and calcareous nannofossil biozonation. *Geologica Acta* **11**, 177–93.

D'Atri, A., Zuffa, G. G., Cavazza, W., Okay, A. I. & Di Vincenzo, G. 2012. Detrital supply from subduction/accretion complexes to the Eocene–Oligocene post-collisional southern Thrace Basin (NW Turkey and NE Greece). *Sedimentary Geology* **243–4**, 117–29.

Doust, H. & Arikan, Y. 1974. The geology of the Thrace Basin. *Proceedings of the 2nd Petroleum Congress of Turkey*, Ankara, 119–36.

Ediger, V. & Alişan, C. 1989. Tertiary fungal and algal palynomorph biostratigraphy of the northern Thrace basin, Turkey. *Revue Palaeobotany and Palynology* **58**, 139–61.

Eleftheriadis, G. & Lippold, H. J. 1984. Altersbestimmungen zum oligozanen Vulkanismus der Süd-Rhodopen/Nord-Griechenland. *Neues Jahrbuch für Geologie und Paleontologie Monatshefte* **3**, 179–91.

Ercan, T., Türkecan, A., Gailou, H., Satir, M., Sevin, D. & Şaroğlu, F. 1998. Features of the Tertiary volcanism around Sea of Marmara. *Bulletin Mineral Research and Exploration* **120**, 97–118.

Erentöz, C. 1949. About the geology of the Çatalca massif and its surroundings (in Turkish). *Istanbul Üniversitesi Fen Fakültesi Mecmuası*; **B14**, 307–20.

Ergintav, S., Demirbağ, E., Ediger, V., Saatçilar, R., İnan, S., Cankurtaranlar, A., Dikbaş, A. & Baş, M. 2011. Structural framework of onshore and offshore Avcılar, Istanbul under the influence of the North Anatolian fault. *Geophysical Journal International* **185**, 93–105.

Gawthorpe, R. L. & Leeder, M. R. 2000. Tectono-sedimentary evolution of active extensional basins. *Basin Research* **12**, 195–218.

Gedik, İ., Timur, E., Umut, M., Bilgin, A. Z., Pehlivan, Ş., Duru, M., Şentürk, K., Özcan, İ. & Çelik, Y. 2014. Geological Maps of Turkey, 1: 50 000 scale Istanbul F21-a sheet and explanatory notes. Ankara: Maden Tetkik ve Arama Genel Müdürlüğü, Ankara, 40 pp.

Georgiev, G. 2012. Geology and hydrocarbon systems in the Western Black Sea. *Turkish Journal of Earth Sciences* **21**, 723–54.

Gökçen, N. 1973. *Etude paleontologique (Ostracodes) et stratigraphique de niveaux du Paleogene du Sud-Est de la Thrace*. Ankara: Maden Tetkik ve Arama Publications, No. 147, 101 pp.

Gradstein, F. M., Ogg, J. G., Schmitz, M. & Ogg, G. 2012. *The Geologic Time Scale 2012*. The Netherlands: Elsevier.

Gültekin, A. H. 1998. Geochemistry and origin of the Oligocene Binkılıç manganese deposit; Thrace Basin, Turkey. *Turkish Journal of Earth Sciences* **7**, 11–23.

Hoşgörmez, H. & Yalçin, M. N. 2005. Gas-source rock correlation in Thrace basin, Turkey. *Marine and Petroleum Geology* **22**, 901–16.

Huvaz, O., Sarikaya, H. & Nohut, Ö. M. 2005. Nature of a regional dogleg pattern in maturity profiles from Thrace basin, northwestern Turkey: A newly discovered unconformity or a thermal anomaly. *American Association of Petroleum Geologists Bulletin* **89**, 1373–96.

İslamoğlu, Y., Harzhauser, M., Gross, M., Jimenez-Moreno, G., Coric, S., Kroh, A., Rögl, F. & van der Made, J. 2008. From Tethys to Eastern Paratethys: Oligocene depositional environments, paleoecology and paleobiogeography of the Thrace Basin (NW Turkey). *International Journal of Earth Sciences* **99**, 183–200.

Juranov, S. 1992. Stratigraphy of the Eocene Series in the Burgas district. *Review of the Bulgarian Geological Society* **53**, 47–59.

Karcioğlu, G., Tank, S. B., Gürer, A., Çiftçi, E. T., Kaya, T. & Tunçer, M. K. 2013. Upper crustal electrical resistivity structures in the vicinity of the Çatalca Fault, Istanbul, Turkey by magnetotelluric data. *Studia Geophysica et Geodaetica* **57**, 292–308.

Kopp, K. O., Pavoni, N. & Schindler, C. 1969. *Geologie Thrakiens IV: Das Ergene Becken*. Geologische Bundesanstalt, Hannover, Beihefte zum Geologischen Jahrbuch no. 76, 136 pp.

Kylander-Clark, A. R. C., Hacker, B. R. & Cottle, J. M. 2013. Laser-ablation split-stream ICP petrochronology. *Chemical Geology* **345**, 99–112.

Lebküchner, R. F. 1974. Beitrag zur Kenntnis des Geologie des Oligozäns von Mittel Thrakien (Türkei). *Bulletin of the Mineral Research and Exploration* **83**, 1–30.

Less, Gy. & Özcan, E. 2012. Bartonian-Priabonian larger benthic foraminiferal events in the Western Tethys. *Austrian Journal of Earth Sciences* **105**, 129–40.

Less, Gy., Özcan, E. & Okay, A. I. 2011. Stratigraphy and larger foraminifera of the Middle Eocene to Lower Oligocene shallow-marine units in the northern and eastern parts of the Thrace Basin, NW Turkey. *Turkish Journal of Earth Sciences* **20**, 793–845.

Menlikli, C., Demirer, A., Sipahioğlu, Ö., Körpe, L. & Aydemir, V. 2009. Exploration plays in the Turkish Black Sea. *The Leading Edge* **28**, 1066–75.

Natal'in, B. & Say, A. G. 2015. Eocene–Oligocene stratigraphy and structural history of the Karaburun area, southwestern Black Sea coast, Turkey: transition from extension to compression. *Geological Magazine* **152**, 1104–22.

Nikishin, A. M., Okay, A. I., Tüysüz, O., Demirer, A., Amelin, N. & Petrov, E. 2015a. The Black Sea basins structure and history: New model based on new deep penetration regional seismic data. Part 1: Basins structure and fill. *Marine and Petroleum Geology* **59**, 638–55.

Nikishin, A. M., Okay, A., Tüysüz, O., Demirer, A., Wannier, M., Amelin, N. & Petrov, E. 2015*b*. The Black Sea basins structure and history: New new model based on new deep penetration regional seismic data. Part 2: Tectonic history and paleogeography. *Marine and Petroleum Geology* **59**, 656–70.

Okay, A. I., Şengör, A. M. C. & Görür, N. 1994. Kinematic history of the opening of the Black Sea and its effect on the surrounding regions. *Geology* **22**, 267–70.

Okay, A. I., Sunal, G., Tüysüz, O., Sherlock, S., Keskin, M. & Kylander-Clark, A. R. C. 2014. Low-pressure–high-temperature metamorphism during extension in a Jurassic magmatic arc, Central Pontides, Turkey. *Journal of Metamorphic Geology* **32**, 49–69.

Oktay, F. Y., Eren, R. H. & Sakinç, M. 1992. Sedimentary geology of the eastern Thrace Oligocene basin in the region of Karaburun-Yeniköy (Istanbul) (in Turkish).

Proceedings of the 9th Petroleum Congress of Turkey, Ankara, 17–21 February 1992, 92–101.

OZANSOY, F. 1962. Les anthrocothériens de l'oligocene inférieur de la Thrace orientale (Turquie). *Bulletin of the Mineral Research and Exploration* **58**, 85–96.

ÖZCAN, E., LESS, GY., BALDI-BEKE, M., KOLLANYI, K. & KERTESZ, B. 2006. Biometric analysis of middle and upper Eocene Discocyclinidae and Orbitoclypeidae (Foraminifera) from Turkey and updated orthophragmine Zonation in the Western Tethys. *Micropaleontology* **52**, 485–520.

ÖZCAN, E., LESS, GY. & KERTÉSZ, B. 2007. Late Ypresian to Middle Lutetian orthophragminid record from central and northern Turkey: Taxonomy and remarks on zonal scheme. *Turkish Journal of Earth Sciences* **16**, 281–321.

ÖZCAN, Z., OKAY, A. I., ÖZCAN, E., HAKYEMEZ, A. & ÖZKAN-ALTINER, S. 2012. Late Cretaceous - Eocene geological evolution of the Pontides in northwest Turkey between the Black Sea coast and Bursa. *Turkish Journal of Earth Sciences* **21**, 933–60.

ÖZGÜL, N. 2012. Stratigraphy and some structural features of the Istanbul Palaeozoic. *Turkish Journal of Earth Sciences* **21**, 817–66.

ÖZTÜRK, H. & FRAKES, L. A. 1995. Sedimentation and diagenesis of an Oligocene manganese deposit in a shallow subbasin of the Paratethys: Thrace Basin, Turkey. *Ore Geology Reviews* **10**, 117–32.

PAPAZZONI, C. A., COSOVIC, V., BRIGUGLIO, A. & DROBNE, K. 2017. Towards a calibrated larger foraminifera biostratigraphic zonation: celebrating 18 years of the application of shallow benthic zones. *Palaios* **32**, 1–5.

PEARSON, P. N., OLSSON, R. K., HUBER, B. T., HEMLEBEN, C. & BERGGREN, W. A. 2006. *Atlas of Eocene planktonic foraminifera*. Cushman Foundation for Foraminiferal Research, Fredericksburg, USA, Special Publication no. 41, 513 pp.

PERINÇEK, D. 1991. Possible strand of the North Anatolian Fault in the Thrace Basin, Turkey: an interpretation. *American Association of Petroleum Geologists Bulletin* **75**, 241–57.

PERINÇEK, D., ATAŞ, N., KARATUT, Ş. & ERENSOY, E. 2015. Geological factors controlling potential of lignite beds within the Danişmen Formation in the Thrace Basin. *Bulletin of the Mineral Research and Exploration* **150**, 77–107.

ROBINSON, A. G., RUDAT, J. H., BANKS, C. J. & WILES, R. L. F. 1996. Petroleum geology of the Black Sea. *Marine and Petroleum Geology* **13**, 195–223.

RODELLI, D., JOVANE, L., ÖZCAN, E., GIORGIONI, M., COCCIONI, R., FRONTALINI, F., SICILIANO, E. R., BROGI, A., CATANZARITI, R., LESS, GY. & ROSTAMI, M. A. 2016. High-resolution integrated magnetobiostratigraphy of a new Middle Eocene section from the southern branch of the Neo-Tethys: Elazığ Basin (Elazığ province, Turkey). AGU poster abstract GP43B-1246, available at: http://adsabs.harvard.edu/abs/2016AGUFMGP43B1246R.

RÖGL, F. 1999. Mediterranean and Paratethys. Facts and hypotheses of an Oligocene to Miocene paleogeography (short overview). *Geologica Carpathica* **50**, 339–49.

ROJKOVIČ, I., SOTÁK, J., KONEČNÝ, P. & ČECH, P. 2008. Stratiform manganese mineralization in the Paleogene and Jurassic shale formations of the Western Carpathians: mineralogy, geochemistry and ore-forming processes. *Geologica Carpathica* **59**, 503–14.

SACHSENHOFER, R. F., STUMMER, B., GEORGIEV, G., DELLMOUR, R., BECHTEL, A., GRATZER, R. & CORIC, S. 2009. Depositional environment and hydrocarbon source potential of the Oligocene Ruslar Formation (Kamchia Depression; Western Black Sea). *Marine and Petroleum Geology* **26**, 57–84.

SAKINÇ, M. 1994. Stratigraphy and paleontology of the Karaburun (Istanbul) marine Oligocene (in Turkish). *Maden Tetkik ve Arama Dergisi* **116**, 9–14.

SANER, S. 1980. Plate tectonic explanation of the basins in the western Pontides and neighbouring areas, northwest Turkey (in Turkish). *Maden Tetkik ve Arama Dergisi* **93**/94, 1–19.

ŞENOL, M. 1980. Depositional environment of Oligocene units and lignite formations in the Keşan (Edirne) and Marmara Ereğlisi (Tekirdağ) regions (in Turkish). *Türkiye Jeoloji Kurumu Bülteni* **23**, 133–40.

SERRA-KIEL, J., HOTTINGER, L., CAUS, E., DROBNE, K., FERRÀNDEZ, C., JAUHRI, A. K., LESS, GY., PAVLOVEC, R., PIGNATTI, J., SAMSO, J. M., SCHAUB, H., SIREL, E., STROUGO, A., TAMBAREAU, Y., TOSQUELLA, J. & ZAKREVSKAYA, E. 1998. Larger foraminiferal biostratigraphy of the Tethyan Paleocene and Eocene. *Bulletin de la Societé Géologique de France* **169**, 281–99.

SINCLAIR, H. D., JURANOV, S. G., GEORGIEV, G., BYRNE, P. & MOUNTNEY, N. P. 1997. The Balkan thrust wedge amd foreland basin of eastern Bulgaria: structural and stratigraphic development. In *Regional and Petroleum Geology of the Black Sea and Surrounding Region* (ed. A. G. Robinson), pp. 91–114. American Association of Petroleum Geologists, Memoir no. 68.

SIYAKO, M. 2006. “Lignitic sandstones” of the Trakya Basin. *Bulletin of the Mineral Research and Exploration* **132**, 63–72.

SIYAKO, M. & HUVAZ, O. 2007. Eocene stratigraphic evolution of the Thrace Basin, Turkey. *Sedimentary Geology* **198**, 75–91.

SOTÁK, J., PERESZLENYI, M., MARSCHALKO, R., MILIČKA, J. & STAREK, D. 2001. Sedimentology and hydrocarbon habitat of the submarine-fan deposits of the central Carpathian Paleogene Basin (NE Slovakia). *Marine and Petroleum Geology* **18**, 87–114.

STEININGER, F. F. & WESSELY, G. 1999. From the Tethyan Ocean to the Paratethys Sea: Oligocene to Neogene stratigraphy, paleogeography and paleobiogeography of the circum-Mediterranean region and the Oligocene to Neogene Basin evolution in Austria. *Mitteilungen der Österreichischen Geologischen Gesellschaft* **92**, 95–116.

SUC, J. P., GILLET, H., ÇAĞATAY, M. N., POPESCU, S.-M., LERICOLAIS, G., ARMIJO, R., MELINTE-DOBRINESCU, M. C., ŞEN, Ş., CLAUZON, G., SAKINÇ, M., ZABCI, C., UCARKUS, G., MEYER, B., ÇAKIR, Z., KARAKAŞ, Ç., JOUANNIC, G. & MACALET, R. 2015. The region of the Strandja Sill (North Turkey) and the Messinian events. *Marine and Petroleum Geology* **66**, 149–64.

TURGUT, S. & ESELLER, G. 2000. Sequence stratigraphy, tectonics and depositional history in Eastern Thrace Basin, NW Turkey. *Marine and Petroleum Geology* **17**, 61–100.

TURGUT, S., TÜRKARSLAN, M. & PERINÇEK, D. 1991. Evolution of the Thrace sedimentary basin and its hydrocarbon prospectivity. In *Generation, Accumulation, and Production of Europe's Hydrocarbons* (ed. A. M. Spencer), pp. 415–37. European Association of Petroleum Geoscientists, Special Publication no. 1.

ÜNAY-BAYRAKTAR, E. 1989. *Rodents from the Middle Oligocene of Turkish Thrace*. Utrecht Micropaleontological Bulletins, Special Publication no. 5, 120 pp.

VARENTSOV, I. M. 2002. Genesis of the Eastern Paratethys manganese ore giants: impact of events at the Eocene/Oligocene boundary. *Ore Geology Reviews* **20**, 65–82.

YURTSEVER, A. & ÇAĞLAYAN, A. 2002. *Geological maps of Turkey, 1. 100 000 scale, Istanbul F21 and G21 sheet and explanatory text*. Ankara: Maden Tetkik ve Arama Genel Müdürlüğü, Ankara, 30 pp.